BLANK PAGE

AFFTC-TR-58-19
ASTIA Document
No. AD 152143
April 1958

Contract No. [illegible](611)-1701

VIBRATION ISOLATION OF HIGH SPEED TRACK VEHICLES

J. C. BURGESS
Stanford Research Institute
Menlo Park, California

AIR FORCE FLIGHT TEST CENTER
EDWARDS AIR FORCE BASE, CALIFORNIA
AIR RESEARCH AND DEVELOPMENT COMMAND
UNITED STATES AIR FORCE

AFFTC-TR-58-19
ASTIA Document
No. AD-152143
April 1958

VIBRATION ISOLATION OF HIGH SPEED TRACK VEHICLES

J. C. Burgess
Stanford Research Institute
Menlo Park, California

April 1958

Contract No. AF 04(611)-1701
SRI Project No. SU-1708

Air Force Flight Test Center
Edwards Air Force Base, California

ACKNOWLEDMENT

Successful accumulation of the data presented in this report is due entirely to the well-organized and enthusiastic efforts of personnel under the direction of Mr. Robert King at the Experimental Track Branch, Air Force Flight Test Center, Edwards Air Force Base, California. Special mention is deserved by Mr. Ernest Coleal, Project Officer, for his guidance of the entire program. Other personnel who made substantial personal contributions are Lt. Charles A Bodeen, (motion picture photography), Mr. Richard A. Acosta (Telemetering), and M/Sgt. David Smyers (design, fabrication, and installation of linkages for sensing spring deflections).

The Institute is indebted to the Hughes Aircraft Company for donation of copies of its IBM-650 routine for generalized harmonic analysis.

CONTRIBUTORS

The research was performed in the Institute's Physical Sciences Division under the direction of Dr. Vincent Salmon, Manager, Sonics and Mechanics Section. Dr. Charles W. Coale and Mr. Hugh L. Smith made substantial contributions to the technical effort.

TABLE OF CONTENTS

TABLE OF CONTENTS (CONTINUED)

TABLE OF CONTENTS (CONTINUED)

LIST OF ILLUSTRATIONS

LIST OF ILLUSTRATIONS (CONTINUED)

LIST OF TABLES

I INTRODUCTION

High-speed track vehicles are extremely important tools in the rapid and economic development of high-speed aircraft and missiles. Their uses include tests of pilot-ejection systems at high velocities, tests of rocket launching systems in the presence of high-velocity cross winds, and development and evaluation tests of inertial guidance systems. The major attractions which track vehicle testing hold for missile and aircraft developers include low operational cost compared with free-flight tests, the amount of control possible over velocity, acceleration, and rate of change of acceleration, the easy repeatability of test conditions, and the recoverability intact of test items and instruments. One of the major limitations of high-speed track vehicles is the noticeably higher vibration environment compared with that of free-flight vehicles.

Personnel at the High-Speed Track Branch of the Air Force Flight Test Center (AFFTC) have taken the initiative in the investigation of track vehicle vibrations and means for their reduction. Under AFFTC sponsorship in 1953, the J. B. Rea Company, Inc., conducted a theoretical investigation[1] of the transient response of vehicle structural components to excitation by rail joints. Following the recommendations of the J. B. Rea Company, personnel of the High-Speed Track Branch conducted an in-house investigation[2] of the effects of spring-damper isolators placed at each vehicle support.

The success of the in-house investigation prompted the AFFTC to request proposals for further research. Stanford Research Institute (SRI) submitted a proposal in January 1956, and was awarded a 12-month contract in March 1956. This is the final report for the contract.

The major objective of the research undertaken by the Institute was to develop criteria for the design of resilient slipper mounts for high-speed track vehicles. Since very little was known about the characteristics of the vibration environment of track vehicles,* the program included investigation of these characteristics as well as development of prototype isolators.

II CONCLUSIONS

Using facilities supplied by the AFFTC, track tests were conducted with a set of resilient slipper mounts (isolators) designed and fabricated at SRI.

---

* A recent paper by Barr and Morrison[3] became available too late to be considered in performing the research reported here.

For the design of resilient slipper mounts, the following criteria are applicable:

1. The isolating mechanism must be designed to operate under the action of downward as well as upward reaction forces at the slipper. Automotive-type suspension systems are thus not directly applicable to track vehicles.

2. The natural frequency of the isolators is fixed by the track operational requirements of (a) a dynamic load factor*, and (b) a maximum allowable verticle displacement of the vehicle.

To fulfill the first of these criteria, cantilever single-leaf springs were chosen. The simplicity of design of the leaf spring and its end connections makes this type of spring very attractive. It is easy to design a fail-safe housing, to install snubbers, to lock out the springs, and to measure spring deflections. The problems of stress and fatigue strength, however, make their use on a permanent basis questionable.

For the AFFTC High-Speed Track, the operational requirements specified in the second design criterion were (a) a 10-g load factor and (b) a maximum allowable vertical vehicle displacement of $\pm$0.25 inch. The corresponding natural frequency is thus 20 cps. Unit dampers were not used with the SRI resilient mounts.

From the data accumulated during the track tests, the following observations can be made:

1. Track irregularities are a major cause of the severe vibration environment of the track vehicle tested. Aerodynamic excitation appears to become important as vehicle velocities increase.

2. Resilient slipper mounts are effective in reducing the contributions of track irregularities to the vehicle vibration environment.

3. Vibration environments at any location in the vehicle are related to the natural frequencies and inherent damping of nearby structural components.

4. Internal damping in the vehicle structure was very high. For the two rigid body modes of vibration allowed (vertical translation and pitching), the equivalent viscous damping is estimated to be between 40 and 80 percent of critical.

---

* The dynamic load factor is expressed in units of g, the acceleration of gravity. A load factor of 10 g means that the dynamic force is ten times the magnitude of the reference force. The reference force used in this report is the weight, or a portion of the weight, of the vehicle.

5. Water brake entry provides the most severe load factors experienced. These range up to almost 20 g. The resultant force exerted on the vehicle by the water brake has a strong vertical component that tends to lift the vehicle off the track. This vertical component is estimated to be between 41,500 and 50,000 lb for a vehicle velocity between 400 and 500 ft/sec.

6. Other than in the water brake, slipper load factors were less than 10 g. Load factors at the slippers induced by rocket onset are not as severe as those induced by rail joints. Load factors induced by rocket burnout are not distinguishable in the spring deflection records.

III RECOMMENDATIONS

A. Investigation of Vibration Environments

As high speed tracks change from butted rails to continuously welded rails, the rail-induced excitation will become less important. Because of rail cross-section variability and track misalignment, however, rail excitation will still exist. In addition, slipper clearances, aerodynamic effects, rocket propulsion, water brake entry, and test-item operation contribute to the vibration environment. The magnitudes and frequency characteristics of these various sources of excitation should be more thoroughly investigated to provide information for vehicle designers.

B. Establishment of Environmental Criteria for Different Types of Track Tests

The environment required for testing inertial guidance components may be completely different from that required for testing pilot-ejection apparatus. A table of environmental criteria should be set up for the vehicle designer.

C. Improved Isolators

The leaf springs used in the prototype SRI isolator functioned as anticipated. Because they are sensitive to stress concentrations, however, they may not be suitable for use under track operation conditions similar to those experienced here. Investigation of other types of resilient mount materials, such as bonded rubber, may reveal one better suited for operational use.

D. Water Brake Redesign

Spring deflection data indicate that peak slipper reactions during the water brake phase are approximately twice as severe as during any other run phase. Indications are that these high reaction forces are caused by an upward force acting on the lip of the water brake scoop. By reducing the severity of this force, greater reliability of vehicle design can be achieved.

IV FACILITIES, TEST PROGRAM, AND INSTRUMENTATION

All test facilities and instrumentation were supplied by the AFFTC. These consisted primarily of the High-Speed Test Track, the test vehicle, telemetering and data transcribing services, accelerometers, and spring deflection transducers.

A. High-Speed Track

The track is 10,000 feet long with rails of standard 39-ft lengths of 115-lb. AREA rail laid with a standard railroad gage of 4ft-8 1/2 in. A water brake trough lies between the rails for the final 2000 ft of track.

B. Test Vehicle

To keep unsteady aerodynamic effects at a minimum, the Radioplane vehicle, "Sh-Boom," was chosen. The relatively clean lines of this vehicle, indicated in Figures 1 and 2, suggest that unsteady shock wave effects may be unimportant. The design of mounting pads for the Radioplane slipper mounts made it an easy matter to design and install other mounts without permanent or expensive change to the vehicle.

The Radioplane vehicle is designed to carry a maximum of seven rocket motors of 11,000 lb thrust each, four in the bottom row (Figure 2) and three in the top row. With seven empty rocket motors, Radioplane slipper mounts, and slippers, the physical constants for the Radioplane vehicle were determined by Air Force personnel to be

$W = 2965$ lb

$\bar{x} = 41.8$ in.

$\bar{y} = 7.8$ in.

$\rho_x = 2.0$ ft

$\rho_z = 4.3$ ft,

where W is the weight of the vehicle, $\bar{x}$ and $\bar{y}$ are distances to the vehicle center of gravity as shown in Figure 3, ρ_x is the radius of gyration about the longitudinal center of gravity axis, and ρ_z is the radius of gyration about the transverse (or lateral) center of gravity axis.

C. Test Program

The test program was designed to show primarily the effects of track irregularities and slipper clearances on the vertical motions of the vehicle. Two sets of track tests were conducted under this program.

The first set was conducted during July 1956. Three runs (Nos. 1, 2, and 3) were made using the Radioplane slipper mounts to check instrumentation locations and to provide data concerning the vibration environment of the unisolated vehicle. The second set was conducted during February 1957. Four runs (Nos. 4, 5, 6, and 7) were made using the SRI resilient slipper mounts. Of these four, two were made with the isolators locked out (Nos. 4 and 7), and two were made with the isolators operative (Nos. 5 and 6).

Five 11,000 lb thrust rocket motors were used for Run No. 1; six rocket motors were used for all other runs. To provide a resultant thrust (F in Figure 3) vector which passes as near to the center of gravity as possible, four rocket motors were located in the bottom row, two in the top row. An empty rocket motor was placed in the center position of the top row for the second set of track tests.

Mechanical failures were few. During Run No. 4, one slipper mount hold-down bolt broke. During Run No. 5, the space-time magnet was knocked off at station 4800. The magnet hit the right rear SRI isolator causing local damage. Also during Run No. 5, screws holding the left front and right rear spring deflection measurement linkages came loose. For Run Nos. 6 and 7, there were no mechanical failures. Water brake entry was observed (by noting water marks beside the track) to be intermittent from stations 8050 to 8150 and to be solid from station 8150 on.

D. Telemetering and Data Transcribing

An FM/FM Bendix-type telemeter system (available at AFFTC) which operates in the 215- to 235-mc frequency band was used for data transmission. The subcarrier range for the various channels is 1.3 to 70 kc. For the SRI tests, 217- and 229-mc carriers were used with subcarriers in the range 2.3 to 22.0 kc. Telemetered data were recorded on an Ampex 500 magnetic tape recorder. Records on oscillograph paper were provided for data reduction.

E. Accelerometers

For Run Nos. 1, 2, and 3, Bendix-type TTO-5 and some Glennite accelerometers were used. For Run Nos. 4, 5, 6, and 7, Statham Model F accelerometers were used. Except at the center of gravity, all accelerometers for the second set of runs were positioned to sense vertical accelerations. At the center of gravity, vertical, transverse, and longitudinal accelerations were sensed. A list of accelerometers used for the second set of runs, their locations, channel information, and frequency response are given in Table I.

Locations of accelerometers for the second set of tests were selected to record the effectiveness of the SRI resilient slipper mounts. Accelerometers were thus located at all four vehicle supports at both slipper and base ends of the springs. Slipper-end accelerometer locations are shown in Figures 4, 5, 8, and 9. The base-end accelerometer location is shown in Figure 6, and the center of gravity accelerometer locations are shown in Figure 7. The accelerometers pictured in Figure 7 were used for the first set of runs. The Statham accelerometers for the second set of runs were mounted on the same bracket.

F. Spring Deflection Transducers

Since spring deflections can be used to obtain the loads which act upon the vehicle, transducers were designed at the AFFTC using Bendix-type TTO-3 position potentiometers as sensing devices. By means of a mechanical linkage, the deflection of the slipper end of each spring with respect to its base end was obtained. This linkage, together with its attachment to the slipper mount, is shown in Figures 8, 9, and 10.

V TRACK VEHICLE DYNAMIC ENVIRONMENT

A. Degrees of Freedom

The track vehicle, as does any structure, has an infinite number of degrees of freedom. For the purpose of this investigation, only three of the six rigid body degrees of freedom have been considered. These are indicated by the coordinates x, y, and θ in Figure 3. The freedoms considered, therefore, correspond to motion along the track, displacement in the vertical direction (vertical translation), and rotation about the transverse center of gravity axis (pitching). The SRI resilient slipper mounts were designed to minimize motion in the other three rigid-body degrees of freedom.

TABLE 1

TRANSDUCER IDENTIFICATION FOR RUN NOS. 4, 5, 6, AND 7

Statham Model F accelerometers were used throughout. Bendix-type TTO-3 position potentiometers were used to sense all four spring deflections.

Location		Transducer		Channel		
Symbol	Description	Range	Cutoff (cps)	mc	kc	Cutoff (cps)
RFD	Right front deflection	± 0.5 in.	--	217	3.9	60
RRD	Right rear deflection	± 0.5 in.	--	229	3.9	60
LFD	Left front deflection	± 0.5 in.	--	217	3.0	45
LRD	Left rear deflection	± 0.5 in.	--	229	3.0	45
CGV	Center of gravity vertical	± 20 g	160	229	10.5	110
CGL	Center of gravity longitudinal	± 20 g	160	217	2.3	35
CGT	Center of gravity transverse	± 20 g	160	229	7.35	110
RFB	Right front base	± 20 g	160	217	14.5	160
RFS	Right front slipper	± 20 g	160	217	22.0	160
RRB	Right rear base	± 20 g	160	217	7.35	110
RRS	Right rear slipper	± 20 g	160	217	10.5	110
LFB	Left front base	± 50 g	280	229	14.5	160
LFS	Left front slipper	± 50 g	280	229	22.0	160
LRB	Left rear base	± 50 g	280	229	5.4	80
LRS	Left rear slipper	± 50 g	280	217	5.4	80

B. Sources of Excitation

The major sources of excitation of a track vehicle are: (1) track irregularities, (2) slipper clearances and insecure attachment, (3) rocket motor noise and unsteady thrust, (4) water brake forces, (5) aerodynamic influences such as unsteady shock wave location, buffeting, and boundary layer noise, and (6) test item operation. The most important sources appear to be track irregularities and slipper clearances. Rocket onset and burnout and water brake entry probably have their major unsteady effects in the low frequency range. Rocket noise and aerodynamic boundary layer noise in general have extremely wide frequency ranges, and their intensities are proportional to a high power of a typical flow velocity. Test item operation is usually not an important source except for such tests as pilot ejection.

C. Gross Motion of the Vehicle

"Gross motion" is used here to designate motion of the vehicle in the x degree of freedom (Figure 3).

The forces which affect the gross motion of the vehicle are those induced by propulsion, aerodynamic drag, and the water brake. For the Radioplane vehicle powered by six 11,000-lb thrust rocket motors, a typical record of the gross motion is given in Figure 11. The dip in the knee of the curve at water brake entry is an effect caused by the use of resilient slipper mounts; hence the dip is not a gross motion effect.

D. Undamped Rigid Body Vibrations

For the two degrees of freedom represented by y and θ in Figure 3, the equations of motion for the free undamped vibrations of the vehicle are

$$m\ddot{y} + 2(k_1 + k_2)y + 2(k_1 b_1 - k_2 b_2)\theta = 0 \qquad (1)$$

$$I_g\ddot{\theta} + 2(k_1 b_1^2 + k_2 b_2^2)\theta + 2(k_1 b_1 - k_2 b_2)y = 0, \qquad (2)$$

where k_1 and k_2 are the spring constants per support.* Equations 1 and 2 indicate that if

$$k_1 b_1 = k_2 b_2, \qquad (3)$$

*Since there are two supports at each end of the vehicle, the total spring constant at each end is 2 k.

the resulting equations of motion would be

$$m\ddot{y} + 2(k_1 + k_2)y = 0 \tag{4}$$

$$I_z\ddot{\theta} + 2(k_1 b_1^2 + k_2 b_2^2)\theta = 0. \tag{5}$$

Since the only dependent variable which appears in Equation 4 is y and the only one which appears in Equation 5 is θ, the motions in the two degrees of freedom are independent of each other. Such motions are spoken of as being "decoupled," and the relation of Equation 3 is the sole requirement in the absence of damping.

The natural frequencies of the decoupled vibrations are given directly from Equations 4 and 5 by

$$(f_n)_y = \frac{1}{2\pi}\sqrt{\frac{2(k_1 + k_2)}{m}} \tag{6}$$

$$(f_n)_\theta = \frac{1}{2\pi}\sqrt{\frac{2(k_1 b_1^2 + k_2 b_2^2)}{m\rho_z^2}}, \tag{7}$$

where the mass moment of interia I_z has been replaced by its equivalent in terms of radius of gyration, ρ_z. Both I_z and ρ_z are taken with respect to the center of gravity z axis.

E. Effects of Damping

Damping can be achieved by several different mechanisms. Perhaps the most common is viscous damping through the use of unit dampers, such as direct acting hydraulic dampers. The use of friction dampers, in which two surfaces are pressed together by either a constant or a variable spring force, is another possibility. If the structure is a flexible one, especially if it has a riveted construction, the damping afforded by minute slippage of joints and fastenings can be responsible for removing a large amount of kinetic energy from the system.

If viscous dampers should be attached at the supports, an additional requirement, similar to Equation 3, can be placed on the damping constants to decouple the damped motions of the vehicle. The resulting decoupled damped modes of vibration are then represented by equations of motion of the type

$$\ddot{y} + 2D\omega_n\dot{y} + \omega_n^2 y = 0, \tag{8}$$

where ω_n is the undamped natural circular frequency and D is the ratio of the (viscous) damping present in the system to the critical damping of the system.

From comparison of the solutions of Equation 8 and either Equation 4 or 5, the ratio of the viscously damped natural frequency to the undamped natural frequency can be found to be

$$\frac{(f_n)\ \text{damped}}{(f_n)\ \text{undamped}} = \sqrt{1 - D^2}\ . \qquad (9)$$

This relation shows that the viscously damped natural frequency is always less than the undamped natural frequency. Calculation using Equation 9 shows that the damped natural frequency is within 10% of the undamped frequency if D is less that 0.44.

The undamped and damped natural frequencies of the isolators selected for the SRI resilient slipper mounts are given in Table II. No damping was intentionally provided for use with the SRI resilient mounts. The records show, however, that considerable damping actually existed. The preceding discussion, therefore, should be considered in terms of "equivalent viscous" damping, where this is defined as the viscous damping that would dissipate the same amount of energy per cycle as the damping actually present.

TABLE II

NATURAL FREQUENCIES OF SRI RESILIENT SLIPPER MOUNTS

Viscous Damping (% Critical)	Frequency			
	Vehicle		Slipper on Spring	
	Vertical Mode (cps)	Rotational Mode (cps)	Front (cps)	Rear (cps)
0	20	26	63	86
40	18.5	24	58	79
60	16	21	50	69
80	12	15.5	38	52

F. Effects of Slipper Mass

The developments in the preceding two subsections are based on the assumption that the slipper end of the spring is directly attached to the "ground." Because of the existence of clearance between the rail and the slipper, this assumption is not correct, although it is a useful one

for preliminary analysis. An adequate investigation of the kinetics of a track test vehicle in which the effects of clearance and of slipper mass are taken into account was beyond the scope of the research reported here.

One possible effect of slipper mass, however, can be easily examined. The weight of the slipper and other components attached to the slipper ends of the SRI springs was measured as 51 lb. If the vehicle end of a spring is considered as built-in, the natural frequency of the slipper mass on the spring can be calculated. These are given in Table II together with the effects on these frequencies of various amounts of viscous damping. Clearance between the slipper and the rail may allow these frequencies to be present.

TABLE III

TYPICAL TRACK JOINT EXCITING FREQUENCIES
(Radioplane Vehicle with Six 11,000-lb Thrust Rocket Motors)

Track Station (ft)	Mean Rail Joint Frequency (cps)	Mean Sled Passage	
		Vertical Mode Excitation (cps)	Rocking Mode Excitation (cps)
400	20	66	33
1,200	32	104	52
3,000	27	88	44
6,000	20	66	33
650	27	88	44
1,750	31	103	52
4,400	24	78	39
7,650	18	58	29

G. Rail Excitation

Effects of the track are felt in three ways: rail joint spacing, spacing between front and rear slippers, and irregularities of the rails themselves.

The most pronounced excitation caused by the track comes from the rail joints. As shown in Figure 11, the rail joint frequency for any run can be

related to the track station since the track station is a unique function of velocity for that run. The rail joint frequency is

$$f_{rj} = \frac{v}{39} \text{ cps}, \tag{10}$$

if v is the vehicle velocity in ft/sec.

Each rail joint gives two impulses to the vehicle, one at the front slippers and one at the rear slippers. For the Radioplane sled with the SRI resilient slipper mounts, the distance between the front and rear slipper pins is 11.75 ft. For the excitation caused by a rail joint striking first the front slippers and then the rear slippers to be in phase with the vertical mode of vibration, the exciting frequency is

$$f_{rjy} = \frac{v}{11.75} \text{ cps}. \tag{11}$$

For the excitation to be in phase with the rotational mode of vibration, the frequency of excitation is

$$f_{rj\theta} = \frac{v}{23.5} \text{ cps}, \tag{12}$$

where v is in ft/sec for both cases.

The exciting frequencies given in Equations 11 and 12 can be put in terms of the rail joint frequency of Equation 10,

$$f_{rjy} = 3.32\, f_{rj}\,, \tag{13}$$

$$f_{rj\theta} = 1.66\, f_{rj}\,, \tag{14}$$

All three of these exciting frequencies are presented in Table III for selected track stations. The rail joint frequency is also indicated in Figure 11.

Irregularities of the track other than rail joints are present. Center line waviness due to incorrect alignment, cross section variation due to rolling-mill tolerances, and changes in both of these due to repeated high load at certain track stations are probably the most important.

VI RESILIENT SLIPPER MOUNT

A. Design Criteria

Several physical criteria govern the design of any realistic resilient mount for a high-speed track vehicle. These are:

1. A low natural frequency

2. A maximum deflection no greater than that considered safe by track operations personnel

3. Ability to withstand the maximum load expected, provision for overload protection, and a built-in fail-safe feature

4. Restriction of vehicle movement to only desired degrees of freedom

5. Incorporation of means of locking out springs.

In addition, the configuration chosen should be easy to manufacture and to install. It should also be rugged and able to withstand the desert environment.

A special requirement is imposed on the physical form of the spring or of the spring mechanism. Since the slippers grip the rails on all sides, downward as well as upward forces are exerted on the vehicle. The situation is thus distinct from that which confronts the automobile designer. Since automobile wheels may leave the ground, the automobile designer must worry only about upward loads acting at the vehicle supports.

B. Selection of Natural Frequencies and Spring Constants

Track operational requirements indicated that a maximum vehicle displacement of $\pm$ 0.25 in. could be allowed. Load factors currently in use prescribed a maximum design load factor of 10 g. The static deflection of the vehicle on the springs was thus

$$\delta_{st} = \frac{0.25}{10} = 0.025 \text{ in.} \tag{15}$$

Since the natural frequency of a single degree of freedom system (or of a decoupled mode of a multi-degree of freedom system) can be given by

$$f_n = \frac{1}{2\pi}\sqrt{\frac{g}{\delta_{st}}} , \tag{16}$$

The natural frequency of the system is fixed by the track operational requirements stated above. Using the value of δ_{st} specified by Equation 15, Equation 16 gives

$$(f_n)_y = 19.8 \text{ cps.} \tag{17}$$

After selecting lengths for the front and rear springs for the SRI resilient slipper mounts, the longitudinal distances from the center of gravity to the slipper pins were

$$b_1 = 92.0 \text{ in.} \tag{18}$$

$$b_2 = 49.0 \text{ in.} , \tag{19}$$

where b_1 and b_2 are as defined in Figure 3.

Using the relations 3, 6, 17, 18, 19, and the information given in Section IV-B, the spring constants for each support can be calculated. These are

$$k_1 = 20,640 \text{ lb/in.} \tag{20}$$

$$k_2 = 38,680 \text{ lb/in.} \tag{21}$$

The frequency in the rocking mode can now be calculated. It is

$$(f_n)_\theta = 25.8 \text{ cps.} \tag{22}$$

Because of uncertainties in manufacture and in damping, the design natural frequencies may be taken as

$$(f_n)_y = 20 \text{ cps}$$

$$(f_n)_\theta = 26 \text{ cps.} \tag{23}$$

C. Types of Spring Available

Several different kinds of spring material and several different forms of spring construction are available. Among the materials are steel, rubber, air, and oil. Among the forms of construction are leaf, helical, and torsion bar springs of steel, sandwich plates and pads of rubber, pneumohydraulic springs (such as those used on the Citroen automobile and in aircraft landing gears), air cushions (such as Firestone Airide springs), and liquid springs (such as those manufactured by the Wales-Strippit Corporation using compressible silicone oils). Mechanical fastenings for helical springs which allow stressing both in tension and compression are extremely difficult to design. The use of helical springs, pneumohydraulic springs, air cushions, and liquid springs is considerably complicated by the mechanism necessary to allow the spring to be stressed in compression while the vehicle is subjected to either an upward or a downward load. These springs could be mounted in pairs so that one is stressed in compression when the load is upward and the other is stressed in compression when the load is downward. In either case, the mechanism necessary would be cumbersome and complicated.

Of the various types of spring investigated, only rubber pads, leaf springs, and torsion bar springs are inherently capable of withstanding both upward and downward loads without the use of complicated linkages or end connections.

D. Leaf Springs for SRI Mount

For the SRI slipper mounts, single-leaf springs were chosen on the basis of simplicity of design of the spring, of the spring fittings, of the snubber and spring lock-out mechanisms, and of the fail-safe spring support. One each of the front and rear leaf springs are shown in Figure 12. As can be seen, the front spring is thinner and shorter than the rear spring. The springs were tapered to provide the greatest deflection possible consistent with the selected design stress. Thus, they approximate beams of constant strength. To reduce stress concentrations at the base and slipper ends, fillets were designed into the spring ends.

The material chosen for these springs was SAE 6150 steel. The springs were machined to almost their final thickness, heat treated, and then ground to the final thickness dimension. Before use, each spring was Magnafluxed at the AFFTC.

The springs were heat treated to Rockwell C 51-53, which corresponds to an ultimate tensile stress between 250,000 and 270,000 psi. Tensile test specimens, heat treated at the same time as the springs, showed an ultimate stress of 261,000 psi. The working stress used for design was 122,500 psi.

In view of the lack of knowledge concerning the maximum stress to be expected in the springs and the number of cycles of this stress per run, resistance to fatigue was not considered in the design of the springs. Stress concentrations were considered in the design, however, so that actual stresses would be within the ultimate strength of the material. Care should be excercised in limiting the number of runs made with these springs because of their unknown resistance to fatigue.

E. Dampers

In the early phases of the program, dampers at each support were thought necessary. Specifically considered were hydraulic dampers. Although a custom-designed damper of the direct-acting type would have been most suitable, the complexity of the design and the cost and time required to fabricate such a custom unit was excessive. Instead, rotary dampers of the Hershey-Houdaille type, which are commercially available, were chosen. Examination and testing indicated, however, that the

maximum damping for the dampers procured was only of the order of 3 to 7% of critical damping. Since this amount was very small compared with the inherent damping expected in the vehicle structure, dampers were omitted.

F. Slipper Mount Design

The design finally selected for the SRI resilient slipper mounts is shown installed on the vehicle in Figures 4 and 5, as well as in other illustrations in this report.

An exploded view of the right front slipper mount is shown in Figure 13. The spring-mount base end (1) is fastened to the vehicle slipper mount pad by six 1/2-in. high-strength bolts. The cover-plate base end (4) is used to fasten the spring (3) to the spring-mount base end (1) by means of another six 1/2-in. high-strength bolts. Four 1/2-in. high-strength bolts are used to fasten the spring (3) to the spring-mount slipper end (9) by means of the cover-plate slipper end (8). All 1/2 in. bolts were tightened by torque-wrench to a torque of 90 lb-ft.

Overload protection is provided by means of the snubber rings (5). These are neoprene rings of suitable hardness which have an inner diameter 1/2 in. greater than the diameter of the slipper pin (10). The snubbers thus allow $\pm$ 1/4 in. free movement of the slipper pin. The snubbers can be compressed another $\pm$ 1/4 in. before the slipper pin will contact the spring-mount base end. Total possible movement of the slipper end of the spring relative to the base end is thus $\pm$ 1/2 in.

To deactivate the spring, the lock-out rings (6) are used in place of the snubber rings (5). The inner diameter of the lock-out rings is only a few thousandths of an inch greater than the diameter of the slipper pins. The ring retainers (7) are used to hold the snubber rings and the lock-out rings in the proper positions on the spring-mount base end. Since the ring retainers must transmit extremely large loads if the springs fail, four close-fitting dowels, visible on the spring-mount base end, are installed with each ring retainer. The four bolts which hold the ring retainers in place do not carry any shear load.

The long ears of the spring-mount base end, together with the high load-carrying ability of the ring retainers, constitute the fail-safe mechanism for these isolators. Stress checks at all critical sections indicate that the slipper mount construction should withstand equivalent static loads of at least 20 g.

Shims (2) are necessary to align the various parts of the slipper mount without causing an initial bending stress in the spring when the spring is locked out. The retaining pins (11) are necessary to prevent the slipper pin from unseating during a run. These pins are safetied in position by ordinary safety wire.

It was necessary to cut a notch in the top rear portion of the slipper (12) so that the spring-mount slipper end (9) would not contact the slipper when heavy downward loads were exerted on the slipper with the springs operative. This cut can be seen in Figure 9.

Positions of the slipper and base-end accelerometers are indicated on the cover-plate slipper end (8) and on the cover-plate base end (7). The displacement gage components can also be seen on the cover-plate slipper end (8) and through the near ring seat of the spring-mount base end (1).

Provision for damper installation was made on the top of the cover-plate slipper end (8). This provision can be seen more clearly in Figure 8. The two vertical ears in the center of the forward end of the cover-plate slipper end were provided for the attachment of a damper arm. In Figure 8, the extension of the spring-mount base end beyond the mounting pad was to have been the mounting spot for the sled-borne part of the damping mechanism.

VII MEASURED VIBRATION AS A FUNCTION OF TRACK STATION

A. Presentation of Data

The classical concept of a vibration environment is one in which the environment consists of one or more discrete sinusoidal frequency components. Examination of most transducer records of actual environments will show, however, that this assumption is an academic one. The vibrational energy is usually spread over a broad and continuous spectrum of frequencies. In addition, specific frequency components that are present usually have amplitudes that vary with time.

Since the actual transducer records usually do not show periodicity, the standard method of harmonic analysis* is not applicable. However, there are methods of analyzing transducer records which are not periodic.

* Harmonic analysis is the resolution of a portion of a record into harmonics of the record length. Thus, only discrete frequency components are found.

The method of primary importance for this report has been called "generalized harmonic analysis." In its graphical form, this method is characterized by a plot of a particular form of "density" of the dependent variable as a function of frequency. The densities used in this report are mean square acceleration density and mean square spring deflection density.

A plot of mean square acceleration density as a function of frequency is called the spectrum of the mean square acceleration density. The integral of this density over any frequency band gives the mean square acceleration for that frequency band. The square root of this integral gives the root mean square (rms) acceleration for the same band width. The band width of the signal analyzed is, therefore, quite important. For example, for a signal the density of which is constant with frequency, the rms acceleration for a band width of 200 cps would be twice the rms acceleration for a band width of only 50 cps.*

The spectra presented in this report were obtained by a punched card routine used with an IBM Type 650 digital computor. This routine was developed by Maso and Drenick[4] of the Hughes Aircraft Company. The basis for this routine is a method developed by John W. Tukey[5] of Princeton University. The Hughes-IBM 650 routine can be used to analyze data for the frequency range 0-1000 cps. Except where noted on the spectra, the data presented in this report were analyzed over the frequency range 0-200 cps. The actual band width is less than 200 cps because of the cut-off frequencies of the telemeter channel filters (see Table I). The pass band of the mathematical filter was 8 cps.

B. Spectra of Vertical Accelerations and Spring Deflections

Records for Run Nos. 3, 6, and 7 were analyzed for mean square acceleration density and, where applicable, mean square spring deflection density (Table IV). Funds were not available for analysis of other run records.

* A more complete discussion of generalized harmonic analysis is beyond the scope of this report. For such a discussion, the reader should see the two reports by Crede[6,7].

TABLE IV

TRACK STATIONS AND RUNS FOR WHICH RECORDS WERE ANALYZED

Station	Run 3	Run 6	Run 7
400	X		
1,200	X		
3,000	X		
6,000	X		
650		X	
1,750		X	X
4,400		X	
7,650		X	

1. Vehicle Center of Gravity, Various Slipper Mounts

For a general look at the effects of slipper mounts with different mechanical impedance characteristics, the vertical acceleration densities at the center of gravity on the Radioplane vehicle are shown in Figure 14. Mean square acceleration density spectra are shown at four different track stations for runs with (a) the Radioplane slipper mounts, (b) SRI slipper mounts with isolators locket out, and (c) SRI slipper mounts with isolators operative. Except for the record at station 1750, the rms acceleration is lowest at each track station when the SRI resilient slipper mounts are operative.

The relatively high level of mean square acceleration density at station 1750 with the isolators operative does not appear to fit with the levels indicated for the other track stations for this run, and probably cannot be explained on the basis of track excitation alone. It may be due in part to the influence of boundary layer (aerodynamic) noise. Since the velocity of the sled is near its peak value and is supersonic at station 1750, boundary layer noise would be more intense than at other stations. The possibility of instrumentation or data reduction error should be considered, also.

It is interesting to note that a reduction in vibration environment is achieved by substituting the SRI slipper mounts with the isolators locked out for the Radioplane slipper mounts. All that can be rationally deduced from this is that SRI slipper mounts with isolators locked out have changed the mechanical impedance of the sled as seen from the slippers and that this change is beneficial.

2. Right Front and Right Rear Supports, Various Slipper Mounts

Figure 15 shows the vibration environments at the right front and right rear supports of the Radioplane vehicle with different supports. Mean square acceleration density spectra are given for track stations near that for maximum velocity (1265 ft/sec) for runs with (a) the Radioplane slipper mounts, (b) SRI slipper mounts with isolators locked out, and (c) SRI slipper mounts with isolators operative. Accelerometers were located at the slipper and base ends of the SRI resilient slipper mounts and at the equivalent base end of the Radioplane slipper mounts.

The spectra in Figure 15 show that at the slipper ends of the SRI springs the rms accelerations are higher with the isolators operative than with the isolators locked out. They show also that the reverse is true at the base ends of the springs. Although the differences are small, the trends are in the directions that would be expected.

More important to assessment of the effects of the springs in the SRI isolators are the spectra at the base ends of the springs and at the equivalent base end of the original Radioplane mounts. Comparison of the two sets of data given in Figure 15 for three types of base end shows that the environment at the base end improves with increasing resilience of the mount. At the front base end, the reductions in rms acceleration is nominal, while at the rear base, the reductions are quite impressive.

3. Front Spring Base, Center of Gravity, and Rear Spring Base, SRI Slipper Mounts

Figure 16 shows that the environment is not the same in all parts of the vehicle. Although some frequency peaks appear in more than one of the spectra, there seems to be very little correlation among the spectra for the three locations in the vehicle at any of the track stations. The primary conclusion to be drawn from this observation is that the assumption of a rigid body must be used with care. Structural flexibilities appear to be important to the vibration environment at localized areas in the vehicle.

4. Right Front and Right Rear Spring Ends, SRI Slipper Mounts

The mean square acceleration densities and mean square spring deflection densities of the right front and right rear SRI slipper mounts are given for various track stations in Figures 17 and 18. These spectra indicate that the acceleration environments at both the slipper and base ends of the front springs are more severe than at the corresponding positions on the rear springs. Across the front spring, the average attenuation of the rms acceleration is approximately 4.4 g. The

corresponding attenuation across the rear spring is approximately 8 g. Apparently, the environment at the front spring is more severe than at the rear spring, and the attenuation experienced at the front spring is not as good as that at the rear spring. The average vibration environment at the base of the front spring appears to be almost five times as severe as that at the base of the rear spring.

C. Resonances

The pronounced frequency peaks visible in most of the spectra presented in Figures 14-18 can provide a lot of interesting conversation. Since the rigid-body undamped natural frequencies of the vehicle are approximately 20 and 26 cps, respectively, (Table II), resonance peaks can be found at or near these frequencies in most of the spectra. Unfortunately, they can be found in the spectra for the Radioplane slipper mounts and for the SRI slipper mounts with the isolators locked out, as well as those spectra obtained with the SRI isolators operative.

There do seem to be some correlation between the track joint exciting frequencies (Table III) and the magnitude of the mean square spring deflection densities. This is particularly noticeable for the spring deflection record at station 7650 feet for the right front isolator (Figure 17). The rail joint exciting frequency at this station is 18 joints per second. As indicated in Table II, 18 cps corresponds to the vertical mode of vibration of the vehicle with approximately 40% critical damping or to the rotational mode with approximately 80% critical damping.

Further efforts to relate peaks indicated in the spectra to resonances of specific structural members, the rigid body motions of the vehicle, or the possible vibrations of the slippers on the ends of the springs are beyond the scope of this report.

D. Aerodynamic Excitation

It is interesting to speculate about the severe vibration environment found at the base end of the front spring since the environments at the center of gravity and at the base of the rear spring are comparatively mild.* Since both front and rear slipper mounts have the same general design, it would seem fair to assume that the attenuations effected should be about the same. Since this is not what happens and since the vibration

* In fact, both of these latter, at all track stations for which records were analyzed, are within the 0.07 g^2/cps maximum vibration level specified by Ramo Wooldridge Corporation[8] for instrument compartments of missiles.

levels at front and rear slippers are about the same, some other source of excitation may be responsible for the more severe than expected vibration level at the base of the front spring.

It is known that aerodynamic noise created by turbulence in fluid boundary layers can be an important source of unsteady excitation for high speed vehicles. Since the clean lines of the Radioplane vehicle were obtained by allowing relatively low transverse stiffness at the front end of the vehicle, it may be that aerodynamic noise is important in exciting resonances due to this low stiffness. At the present time, no proof exists that this is or is not the case. Future experimental work should be designed to throw more light in this direction.

VIII LOADS ACTING AT VEHICLE SUPPORTS

A. Presentation of Data

The oscillograph records for the signals from the spring deflection gages have been traced and gage calibrations provided for those tracings from Run No. 6. These tracings are presented in Figures 19 and 20. They were picked to show the vibration effects on the vehicle from rocket firing, rocket burnout, water brake entry, and rail joint excitation. For correlation, deflection gage records are provided for the same track stations for which spectra were calculated (Figures 17 and 18). The spring deflection records thus give the loads exerted at the base ends of the the four springs. They also show the motion of the vehicle in the various rigid body modes of vibration.

The datum lines are the prerun zeros; postrun zeros are shown at the right for those channels which had dependable postrun zeros. The postrun zeros obtained for the deflection gages were close to the prerun values for only three out of eight channels possible (for two runs). Load data in some cases are thus questionable, since a small change in zero position corresponds to a significant change in load. The effects of propellant weight upon the differences between prerun and postrun zeros are small, corresponding to load factors less than 0.4 g. The poor postrun zeros obtained for the rear deflection gages were undoubtedly caused by grounding due to spray from the water brake.

The following sign convention has been adopted to describe spring deflections and loads. Upward acting loads and upward movements of the spring base (hence the vehicle) from the position of static equilibrium are assumed positive and are given the (+) sign. Thus the lowering of the vehicle corresponds to a minus (-) deflection and to an upwards (+) reaction on the vehicle.

B. Static and Semisteady Slipper Reactions

The propulsion, aerodynamic, and water brake forces which act on the vehicle have measurable steady or semisteady components as well as oscillating components. Although a thorough investigation of these forces is beyond the scope of this report, the spring deflection data are so closely related to slipper reaction forces that some discussion of this subject is warranted.

1. Calculated Reactions

For the Radioplane vehicle with seven empty rocket motors and SRI resilient slipper mounts in place, the static loads on the slippers are calculated to be (see Figure 3)

$$\left.\begin{aligned} R_1 &= 516 \text{ lb/slipper} \\ R_2 &= 967 \text{ lb/slipper} . \end{aligned}\right\} \quad \text{Rocket motors empty} \tag{24}$$

At the beginning of the run, the propellant weight affects the static reactions somewhat. With six full rocket motors, the reactions at the supports would be approximately

$$\left.\begin{aligned} R_1 &= 616 \text{ lb/slipper} \\ R_2 &= 1,296 \text{ lb/slipper} . \end{aligned}\right\} \quad \text{Six rocket motors full} \tag{25}$$

The rocket-empty reactions given in Equation 24 were used in calculating the spring constants required for decoupling the natural modes of vibration. Thus these reactions (Equation 24) correspond to static deflections of 0.025 in. for each spring.

By neglecting aerodynamic and friction forces between slippers and rails, the effects of rocket thrust on slipper reactions can be calculated. With four rocket motors in the bottom row and two in the upper row, the moment arm of the resultant rocket thrust is (see Figure 3)

$$h_t = 12.1 \text{ in.} \tag{26}$$

Using the nominal value for thrust per rocket, 11,000 lb, the slipper reactions are

$$\begin{aligned} R_1 &= 1,521 \text{ lb/slipper} \\ R_2 &= -38 \text{ lb/slipper} \end{aligned} \tag{27}$$

In terms of load factors based on Equation 24, these reactions are

$$R_1 = +3.0\ g$$

$$R_2 = -0.04\ g\ . \qquad (28)$$

2. Experimentally Determined Reactions

In Table V are given the approximate average spring deflections for the various sections of the oscillograph records presented in Figures 19 and 20. Also given are the corresponding approximate load factors.

TABLE V

SEMISTEADY SPRING DEFLECTIONS AND SLIPPER REACTION LOAD FACTORS
(Run No. 6)

Note: Sign convention - upward vehicle displacement, upward reactions are (+)

Phase of Run	Track Station (ft)	Approximate Vehicle Velocity (ft/sec)	Average Spring Deflections		Approximate Slipper Reactions	
			Front (in.)	Rear (in.)	Front (g)	Rear (g)
Rockets burning	25	0+	-0.14	+0.01*	+5.6	- 0.4*
Rockets burning	650	1,000	-0.21	+0.05*	+8.4	- 2.0*
Coast	1750	1,200	+0.01	+0.09*	-0.4	- 3.6*
Coast	4400	900	-0.02	+0.04*	+0.8	- 1.6*
Coast	7650	680	-0.01	+0.03*	+0.4	- 1.2*
Water brake	8400	500	+0.10	+0.32*	-4.0	-12.8*
Postrun zero	--	--	0	+0.07*	0	- 2.8*

* Postrun zero available only for right rear, and this one is poor. Data questionable

Just after rocket onset, the measured load factor for the front spring force is + 5.6 g--almost twice the value calculated above. Both are average values and do not take into account the effects of rocket onset. The most plausible cause for the discrepancy appears to be inaccurate calibration of spring deflection vs oscillograph trace deflection.

By the time the vehicle has reached a velocity of approximately 1,000 ft/sec, the upward load factor of the front supports has increased by 2.8 g and that at the rear supports has decreased (algebraically speaking) by 1.6 g. These load factors correspond to an increase of approximately 2,900 lb in the upward reaction on the two front supports and an increase of approximately 3,100 lb in the downward reaction at the rear supports. The net change in vertical force on the vehicle is thus near zero. The change in the reaction forces can probably be attributed to aerodynamic loads distributed so that a moment is created, tending to rotate the front of the vehicle downward. A glance at Figure 2 indicates that the assumption of such aerodynamic loads is a sensible one for subsonic flows.

Due to the uncertainty of the postrun zeros for both rear springs, little can be said about the average slipper reactions during the coast phase of the run. However, there does seem to be a noticeable difference between the reactions during the supersonic and subsonic portions of the coast phase. For the supersonic portions of the run (station 1750), it would appear (see Table V) that a net downward reaction force acts on the vehicle at the four vehicle supports. Because of the undependability of the rear spring postrun zeros, the best that can be said is that these reactions correspond to a net aerodynamic lift (i.e., upward) force somewhere between 3,000 and 12,000 lb. For the subsonic portions of the run (stations 4400 and 7650), it appears that an aerodynamic moment exists which tends to force down the front of the vehicle. This observation is in agreement with that noted for station 650 with the rockets burning.

The data for water brake entry are somewhat surprising. Ordinary assumptions concerning the forces on the water brake would indicate a downward force on the vehicle. The spring deflection data clearly show that instead a very strong upward force exists. The net upward force exerted on the vehicle by the water brake is probably between 41,500 and 50,000 lb.

C. Starting Transient, Rocket Burnout, and Water Brake Entry

For the track tests of the SRI isolators, sudden loads were applied at rocket onset, rocket burnout, and water brake entry. To illustrate the transient effects on the vehicle, the spring deflection records for these three portions of Run No. 6 are shown in Figure 19. The corresponding maximum and minimum spring deflections and slipper reaction load factors are listed in Tables VI and VII.

TABLE VI

MAXIMUM AND MINIMUM SPRING DEFLECTIONS AT VARIOUS TRACK STATIONS (Run No. 6)

Note: Sign convention - - upward displacement of vehicle corresponds to (+) spring deflection

Track Station (ft)	Deflection			
	Front		Rear	
	Right (in)	Left (in)	Right (in)	Left (in)
Starting Transient (0-30)	0	+0.03	+0.04	+0.08
	-0.19	-0.22	-0.07	-0.02
0-500	0	+0.03	+0.26	+0.13
	-0.26	-0.27	-0.10	-0.05
650-1150	-0.13	-0.14	+0.10	+0.16
	-0.24	-0.25	0	+0.06
Rocket Burnout (1300-1750)	+0.07	+0.08	+0.19	+0.22
	-0.10	-0.16	+0.04	+0.04
1750-2300	+0.05	+0.14	+0.21	+0.18
	-0.10	-0.05	+0.03	+0.03
4400-4850	+0.07	+0.07	+0.15	+0.15
	-0.14	-0.12	-0.05	-0.03
7650-8000	+0.07	+0.07	+0.16	+0.11
	-0.12	-0.11	+0.02	-0.05
Water Brake Entry 8000-8100	+0.22	+0.22	+0.34	+0.29
	-0.24	-0.27	-0.18	-0.19
8100-8500	+0.23	+0.27	+0.54	+0.40
	-0.07	-0.08	+0.03	-0.03
Postrun Zero	-0.01	+0.01	+0.07	None

TABLE VII

MAXIMUM AND MINIMUM SLIPPER LOAD FACTORS AT VARIOUS TRACK STATIONS
(Run No. 6)

Note: Sign convention: Upward reactions are (+)

Track Station (ft)	Load Factors			
	Front		Rear	
	Right (g)	Left (g)	Right (g)	Left (g)
Starting Transient (0-30)	0	- 1.2	- 1.6	- 3.2
	+ 7.6	+ 8.8	+ 2.8	+ 0.8
0-500	0	- 1.2	-10.4	- 5.2
	+10.4	+10.8	+ 4.0	+ 2.0
650-1150	+ 5.2	+ 5.6	- 4.0	- 6.4
	+ 9.6	+10.0	0	- 2.4
Rocket Burnout (1300-1750)	- 2.8	- 3.2	- 7.6	- 8.8
	+ 4.0	+ 6.4	- 1.6	- 1.6
1750-2300	- 2.0	- 5.6	- 8.4	- 7.2
	+ 4.0	+ 2.0	- 1.2	- 1.2
4400-4850	- 2.8	- 2.8	- 6.0	- 6.0
	+ 5.6	+ 4.8	+ 2.0	+ 1.2
7650-8000	- 2.8	- 2.8	- 6.4	- 4.4
	+ 4.8	+ 4.4	- 0.8	+ 2.0
Water Brake Entry 8000-8100	- 8.8	- 8.8	-13.6	-11.6
	+ 9.6	+10.8	+ 7.2	+ 7.6
8100-8500	- 9.2	-10.8	-21.6	-16.0
	+ 2.8	+ 3.2	- 1.2	+ 1.2
Postrun Zero	+ 0.4	- 0.4	- 2.8	?

Although rocket onset causes a brief transient disturbance to the vehicle, the slipper reactions are not as great as those caused by rail joints in the first 500 feet of track. Rocket burnout causes no transient disturbance that can be distinguished as such.

Water brake entry provided the most severe test of the strength of the SRI slipper mounts and of the vehicle of any portion of the run. Maximum load factors were very severe, reaching a peak value of approximately -18.8 g* for the right rear support at approximately Station 8300.

The oscillograph traces for the rear spring deflections indicate two oscillation build-ups, the first starting at 8,000 feet and the second at 8,100 feet. Visual observation of water marks beside the water brake area following this run indicated intermittent water brake entry from 8,050 to 8,150 feet and full entry from 8,150 on.

In view of the data now available, which show that the water brake exerts a net upward force on the vehicle, skipping of the water brake before full entry may mean that the upward force comes from the lip of the brake scoop. Since the severe loads placed upon the vehicle by the steady and transient effects of this strong upward-acting force pose the most stringent strength requirements on the vehicle structure of any phase of the test run, further investigation of the effects of lip shape are fully warranted.

D. Effects of Rail Joints and Track Irregularities

For the most part, the effects of the rail joints are hidden in the records. It is only at low vehicle velocities that explicit effects of rail joints can be seen. In Figure 19 (a), spring deflections caused by the first four rail joints are clearly visible. Since the vehicle is almost 12 feet long, the indications for the rear springs occur later in time than those for the front springs.

By referring to Table III for track joint exciting frequencies and then thumbing through the spectra in Figures 14-18, occasional evidence of rail joint excitation can be seen. Perhaps the most pronounced evidence from the spectra comes from the increased spring deflection densities when the rail joint exciting frequency is near one of the natural frequencies of the vehicle. The spectra and spring deflection traces can be correlated fairly well in this respect at Stations 4400 and 7650. The complete records show rather uniform oscillation response of the vehicle in the entire range from about Station 4000 to water brake entry.

* -21.6 + 2.8

A more general observation can be made from a study of the spring deflection records shown in Figure 20. The corresponding portions of the records for Run Nos. 6 and 5 are shown in this figure. Although superficial differences exist, the similarities of the records for each spring as a function of track station become more and more striking the longer the records are studied. These similarities create an extremely strong inference that the motion of the vehicle is controlled mostly by track irregularities. In examining these deflection records, it is interesting to note that the times of arrival at various track stations are different for the two runs. The characteristics of the spring deflection curves are thus more firmly established as being functions of track station.

A particularly interesting observation can be made from the spring deflection records in Figure 19 (c). From Station 8350 to 8500, the records for both right springs are fairly smooth while the records for both left springs are relatively erratic. These suggest that the rail heads on the right side of the track are a good deal rougher than those on the left side of the track. Because the slipper reactions on the vehicle are downward-acting at these stations, the slippers are, of course, riding on the underside of the rail heads.

E. Oscillatory Motions of the Vehicle

The motions of the vehicle in its rigid body modes of vibration can be inferred from the spring deflection records of Figures 19 and 20. In the water brake, for example, a severe oscillation is set up in the pitching mode. This pitching oscillation persists until the water brake has fully entered the water, at about Station 8300.

These records help verify one of the assumptions made concerning the motion of the vehicle -- that the rolling mode is not important. The records show that, in most cases, both front springs and both rear springs act together. When differences between right and left spring deflections occur, the track itself may be responsible. The similarities between the records for Run Nos. 5 and 6 (Figure 20) tend to strengthen this belief.

F. Damping

As mentioned in Section VI-E, no damping was intentionally provided for the track tests with SRI isolators. The records indicate, however, that considerable damping was present. The rapidity with which the rocket onset and rail joint transients shown in Figure 19 (a) die out is one of the indications of this high damping capacity. Very rough estimates place the equivalent viscous damping in the range of 40-80% of critical damping for either pitching or vertical translation modes of oscillation.

There are probably three mechanisms present through which this high damping capacity arises. First, the structure itself has many riveted joints which can dissipate energy by friction.* Second, the structure has many resonant structural parts, and energy from the rigid body motions can be transmitted through the structure to these resonant parts. The kinetic energy thus transferred is lost to the primary oscillating system. The action is somewhat similar to that of a dynamic vibration absorber. Third, the design of SRI slipper mounts may allow friction forces to exist. There is a close fit between the ears of the spring-mount slipper end (item 9 in Figure 13) and the ears of the spring-mount base end (item 1 in Figure 13). Transverse forces at the slippers may create high normal forces and hence dry friction effects.

* This observation suggests that riveted vehicles may have a significant advantage over welded vehicles.

REFERENCES

1. Hiroskige, Y. and C. G. Simpson, The Theoretical Investigation of Sled Vibration Problems During Testing and Braking Periods, The J. B. Rea Company, Inc., Los Angeles. Final Report, Contract AF 04(611)-420, Sept. 15, 1953.

2. Coleal, E. Investigation of the Use of Shock Isolation Systems for High-Speed Track Research Testing, Air Force Flight Test Center, Edwards Air Force Base, California, AFFTC-TN-57-12, April 1957.

3. Barr, G. M., and S. C. Morrison, Measurements of the Vibration Environment in a Supersonic Liquid-Propellant Rocket Sled, Paper No. 416-57 presented at The American Rocket Society Meeting, Washington, D. C., April 4-6, 1957.

4. Maso, E., and W. J. Drenick, The Determination of the Autocorrelation and Power Spectrum by Use of the IBM-Type 650, IBM Tech. Newsletter No. 10, Oct. 1955, p 142.

5. Tukey, J. W., The Sampling Spectrum of Power Spectrum Estimates, Symposium on Applications of Autocorrelation Analysis to Physical Problems, Office of Naval Research, p 47.

6. Crede, C. E., Vibration and Vibration Isolation in Aircraft and Guided Missiles, Barry Controls Inc., Watertown, Mass., Report No. 257a, Nov. 25, 1955.

7. Crede, C. E., and E. J. Lunney, Establishment of Vibration and Shock Tests for Missile Electronics as Derived from the Measured Environment, Barry Controls, Inc., Watertown, Mass., WADC Tech. Rep. 56-503 (Contract AF 33(616)-2188) December 1, 1956.

8. Airborne Guidance and Control Equipment, WS 107A and WS315A, Environmental Test Requirements, Guided Missile Research Division, Ramo Wooldridge Corporation, Los Angeles, No. GM 43.5-40, August 20, 1956, p 6.

Figure 1 Radioplane Vehicle "Sh-
Boom, Front Quarter View.

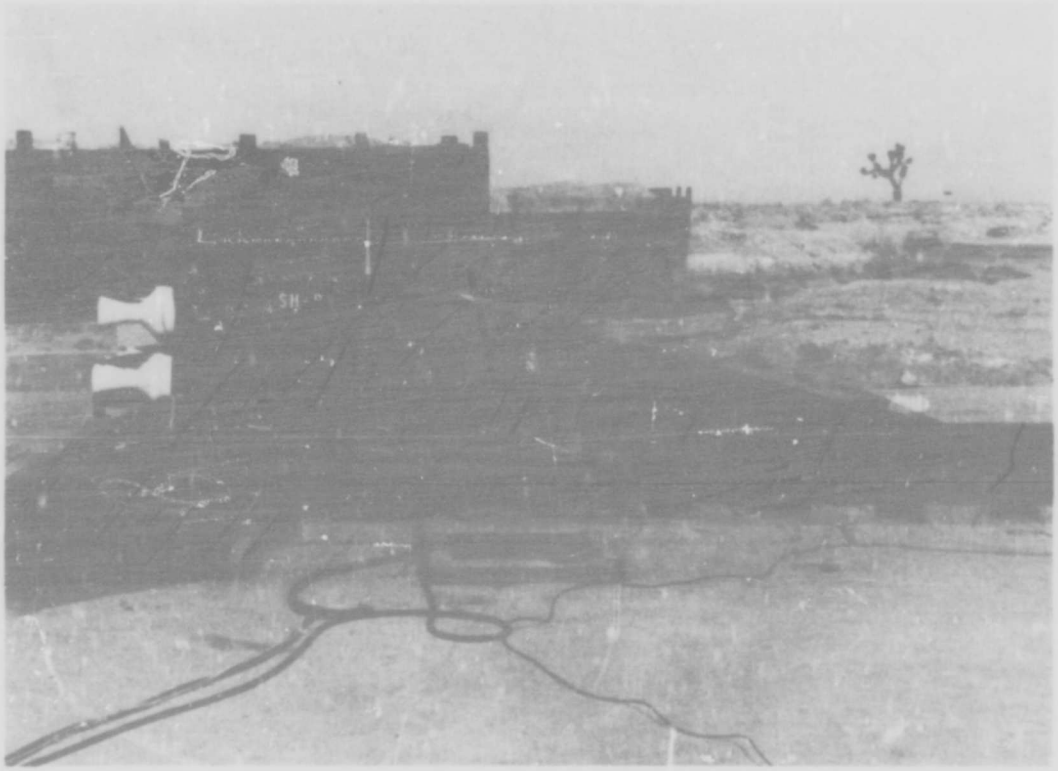

Figure 2 Radioplane Vehicle "Sh-Boom", Side View.

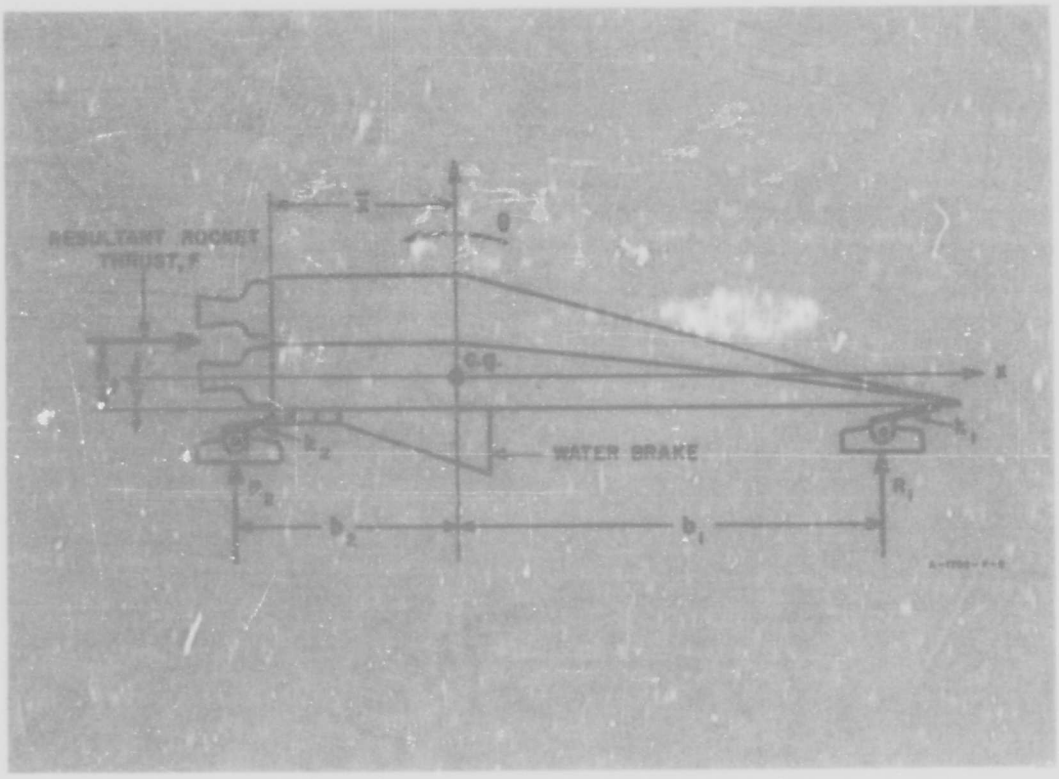

Figure 3 Radioplane Vehicle with Resilient Mounts; Sketch Showing Center of Gravity and Important Dimensions.

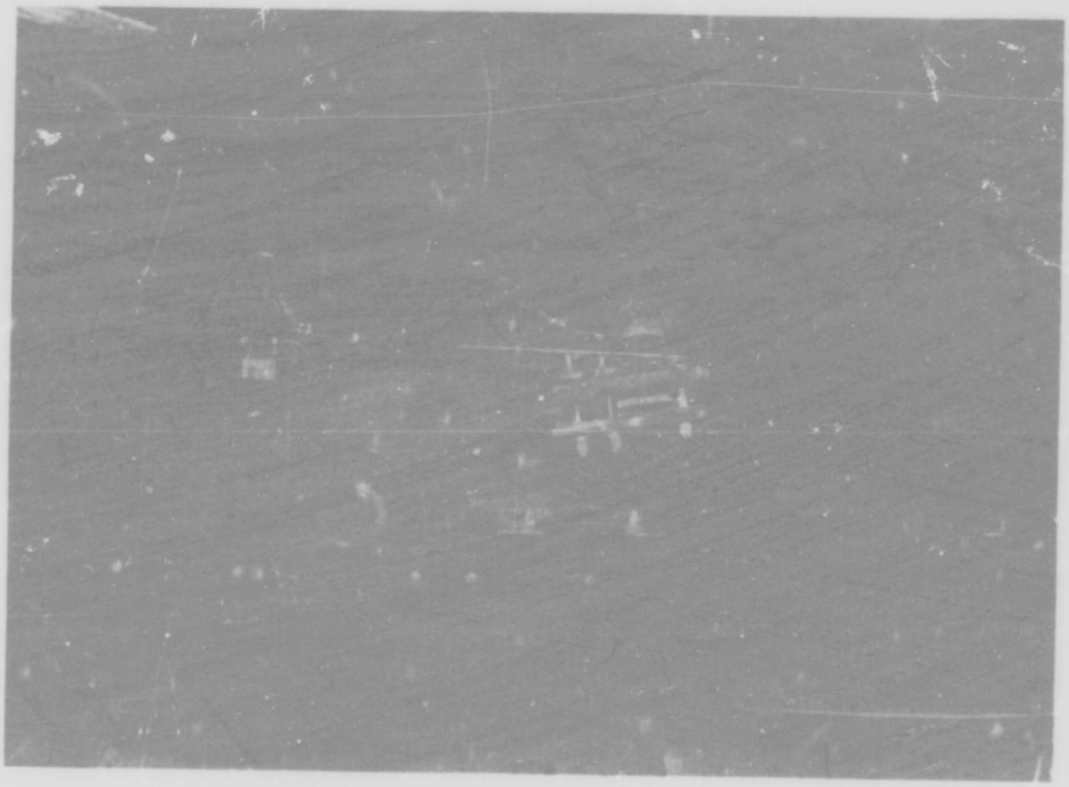

Figure 4 SRI Resilient Slipper Mount, Right Front.

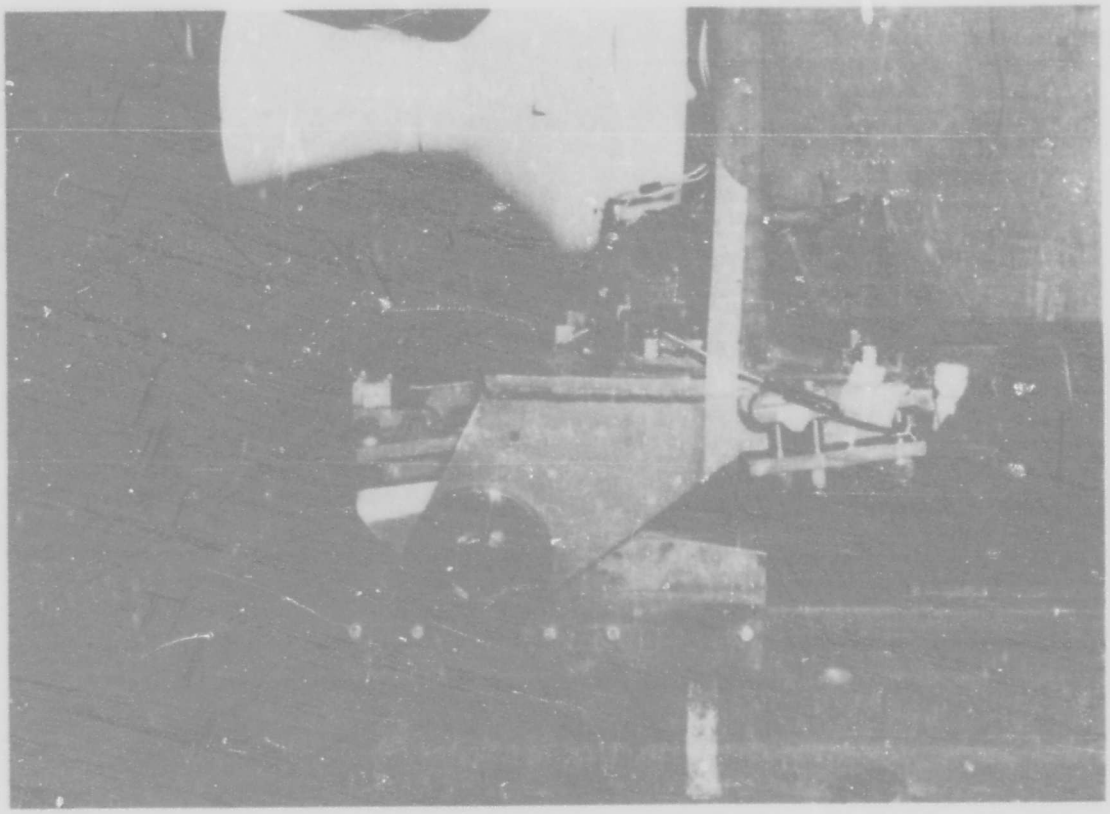

Figure 5 SRI Resilient Slipper Mount, Right Rear.

Figure 6 SRI Left Rear Slipper Mount, showing "Left Rear Base" Accelerometer.

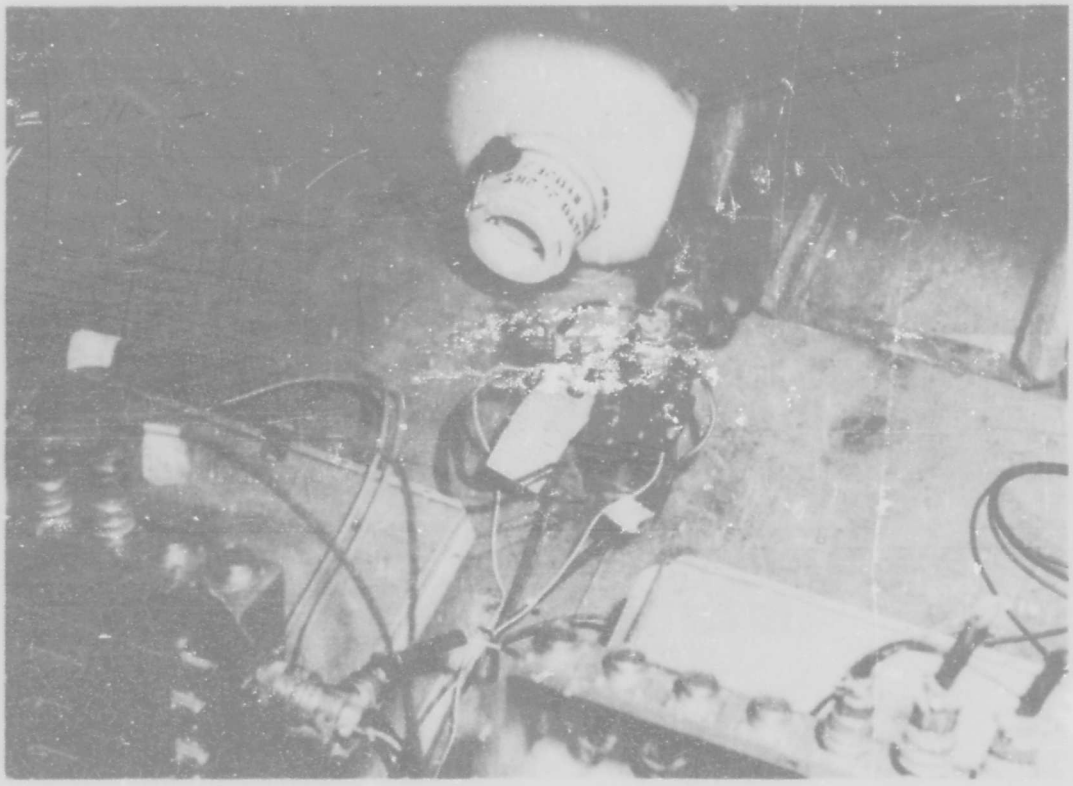

Figure 7 Accelerometers at Vehicle Center of Gravity

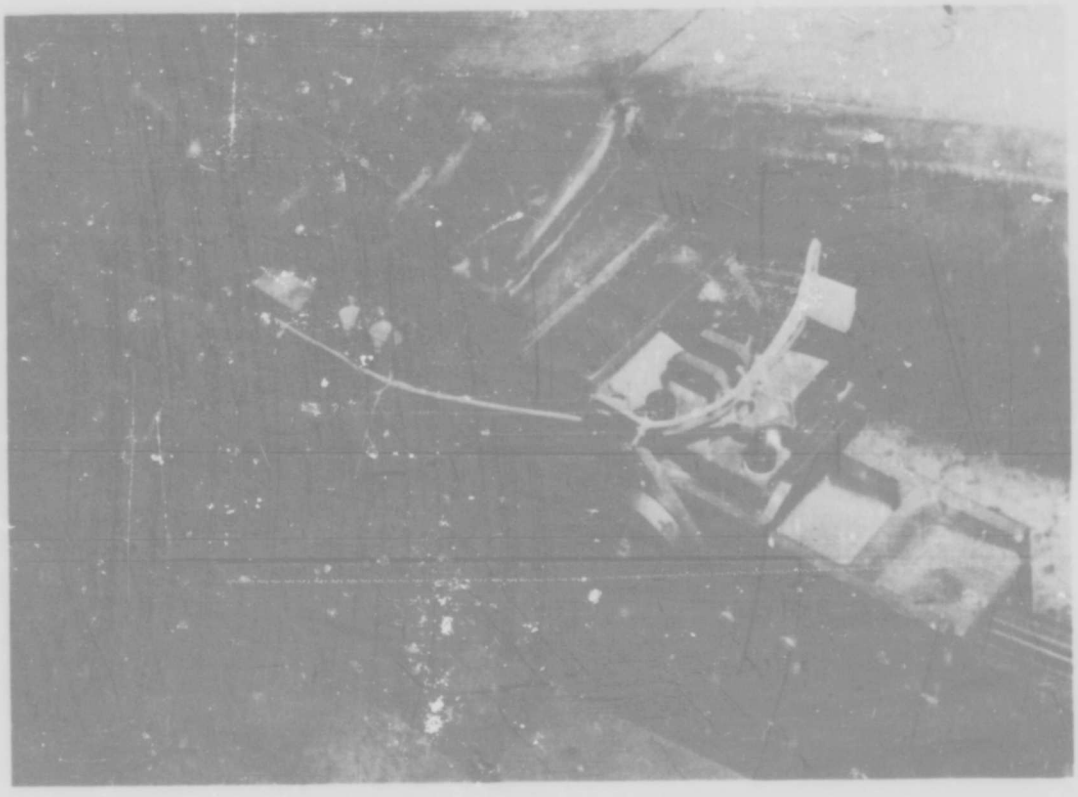

Figure 8 SRI Left Front Slipper Mount. Showing "Left Front Slipper" Accelerometer and "Left Front Displacement" Potentiometer.

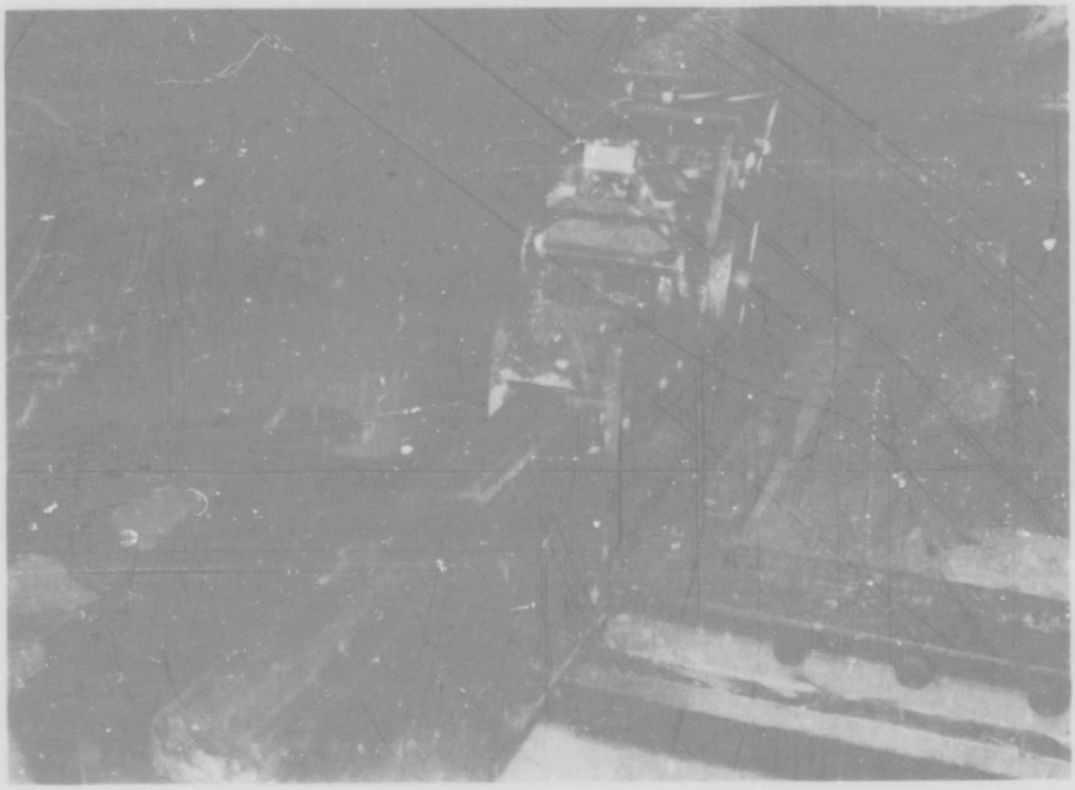

Figure 9 SRI Left Rear Slipper Mount.

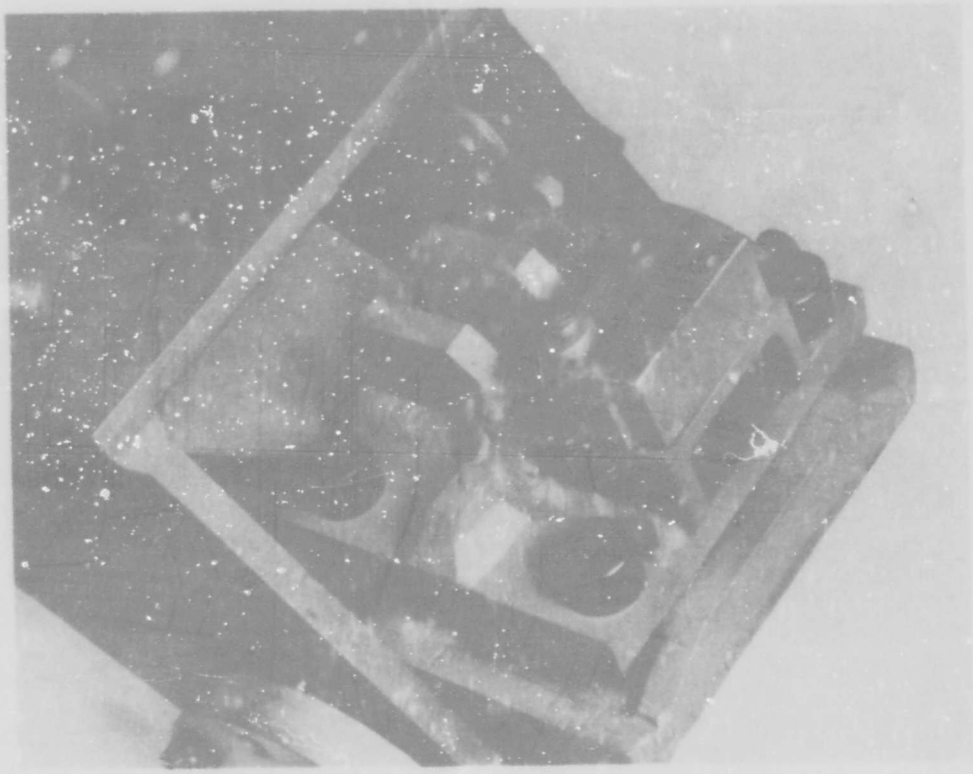

Figure 10 Closeup View of "Left Front Displacement" Position Potentiometer and its Linkage.

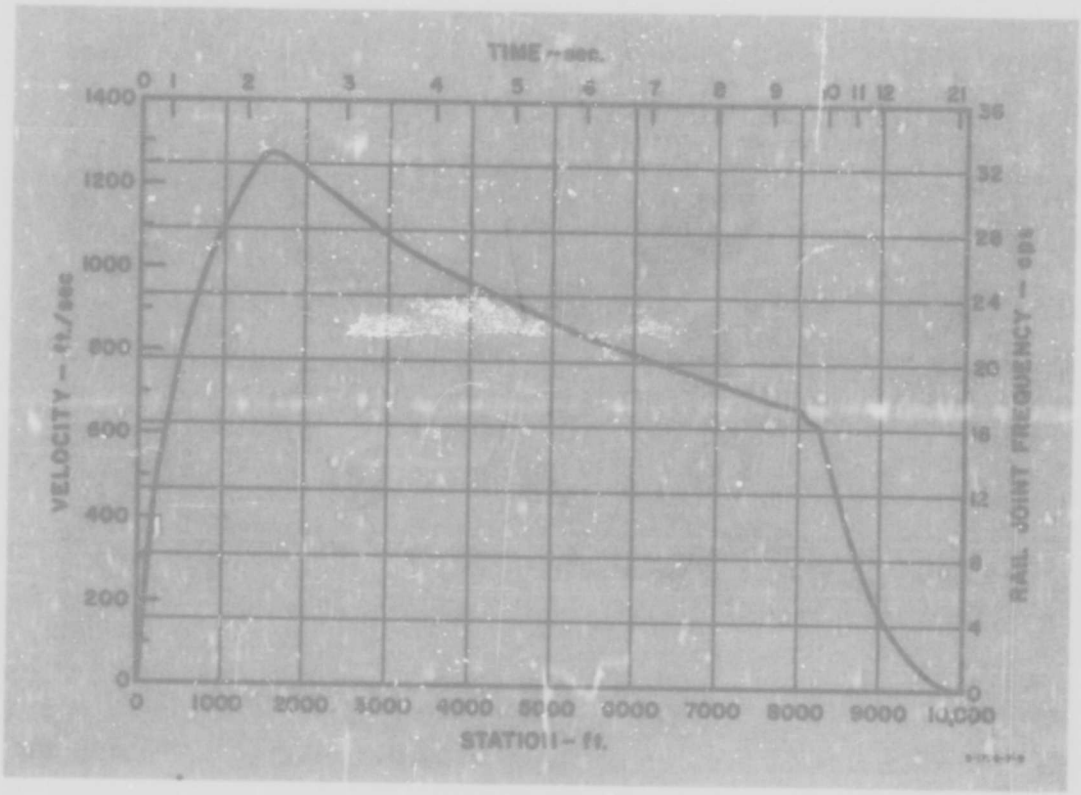

Figure 11 Typical Velocity and Rail Joint Frequency vs Station and Time Curve for Radioplane Sled with Six 11,000-lb Thrust Rocket Motors.

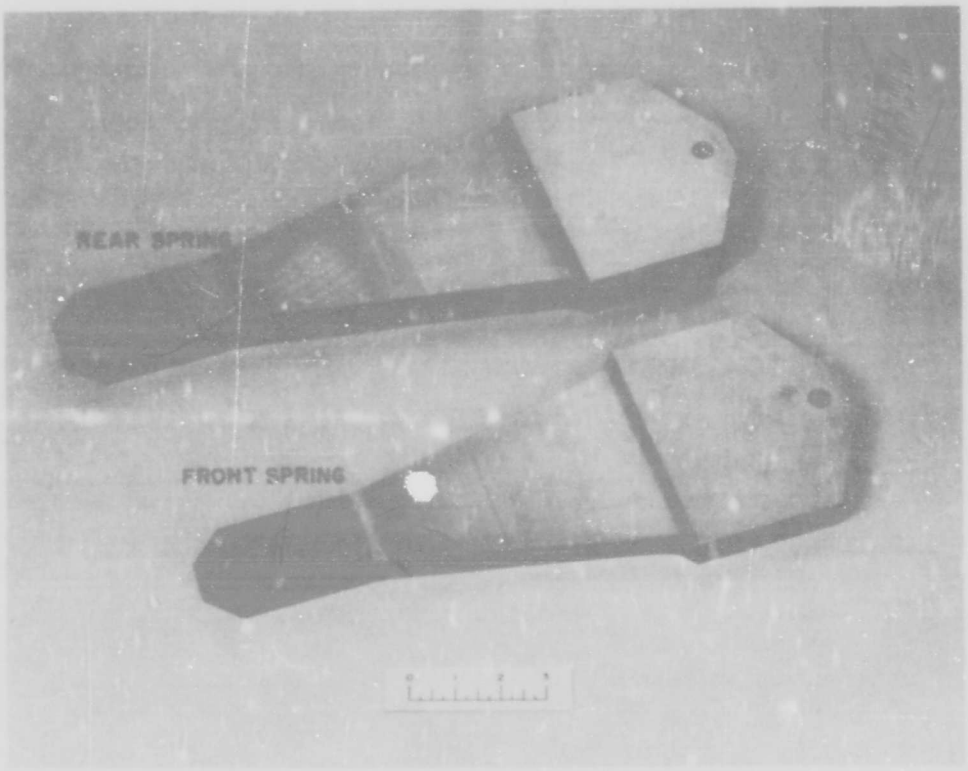

Figure 12 Single Leaf Springs for SRI Slipper Mount.

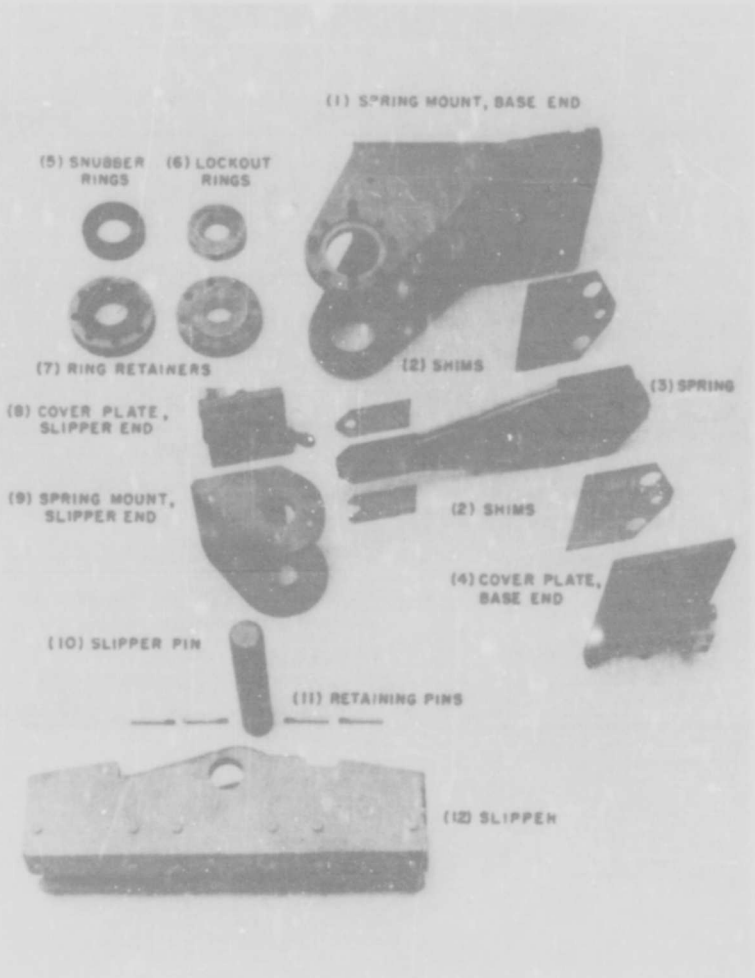

Figure 13 Exploded View of Right Front SRI Slipper Mount.

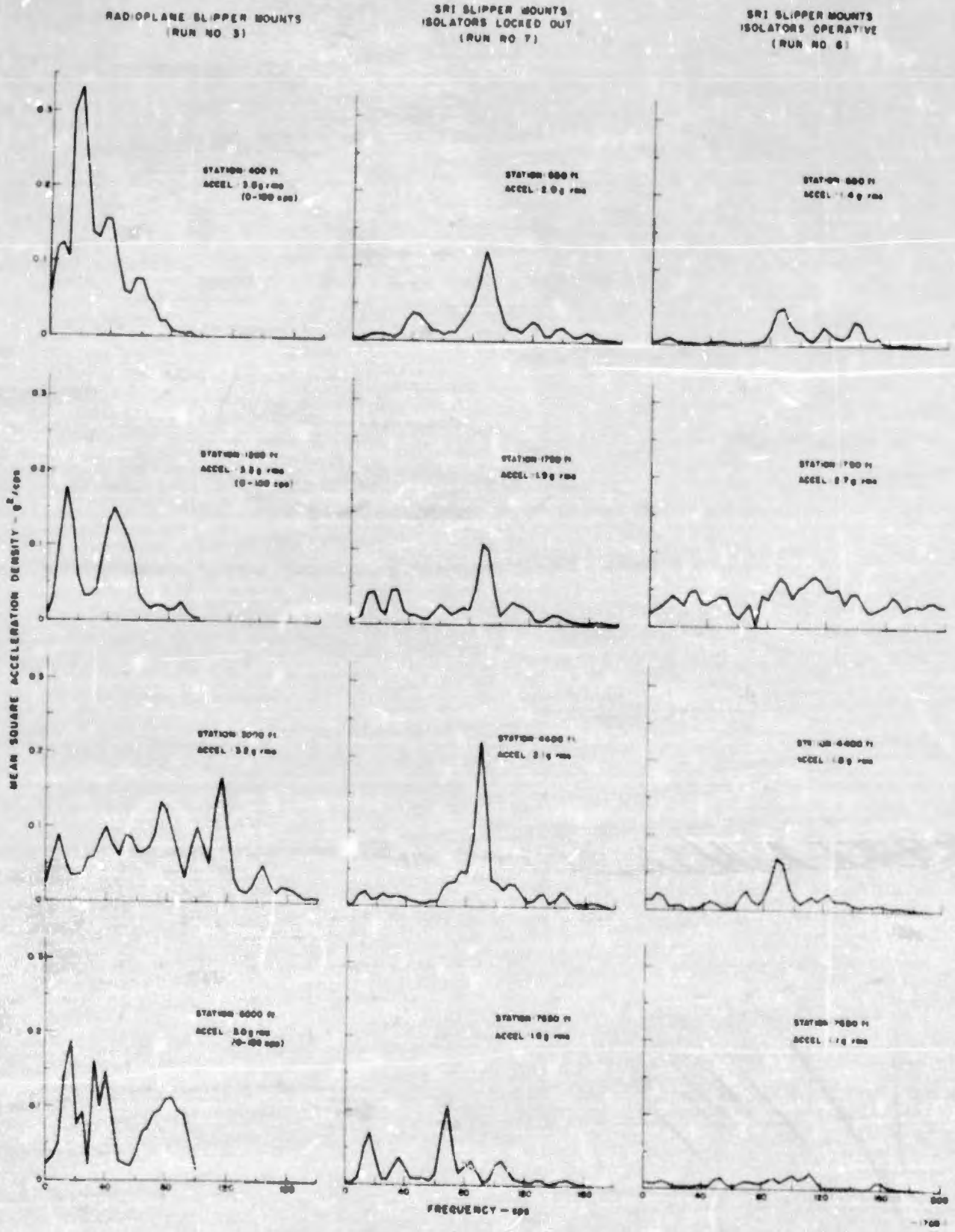

Figure 14 Spectra of Mean Square Acceleration Density at Various Track Stations for Radioplane Sled with Three Types of Slipper Mount; Accelerometer, Vertical Direction at Center of Gravity.

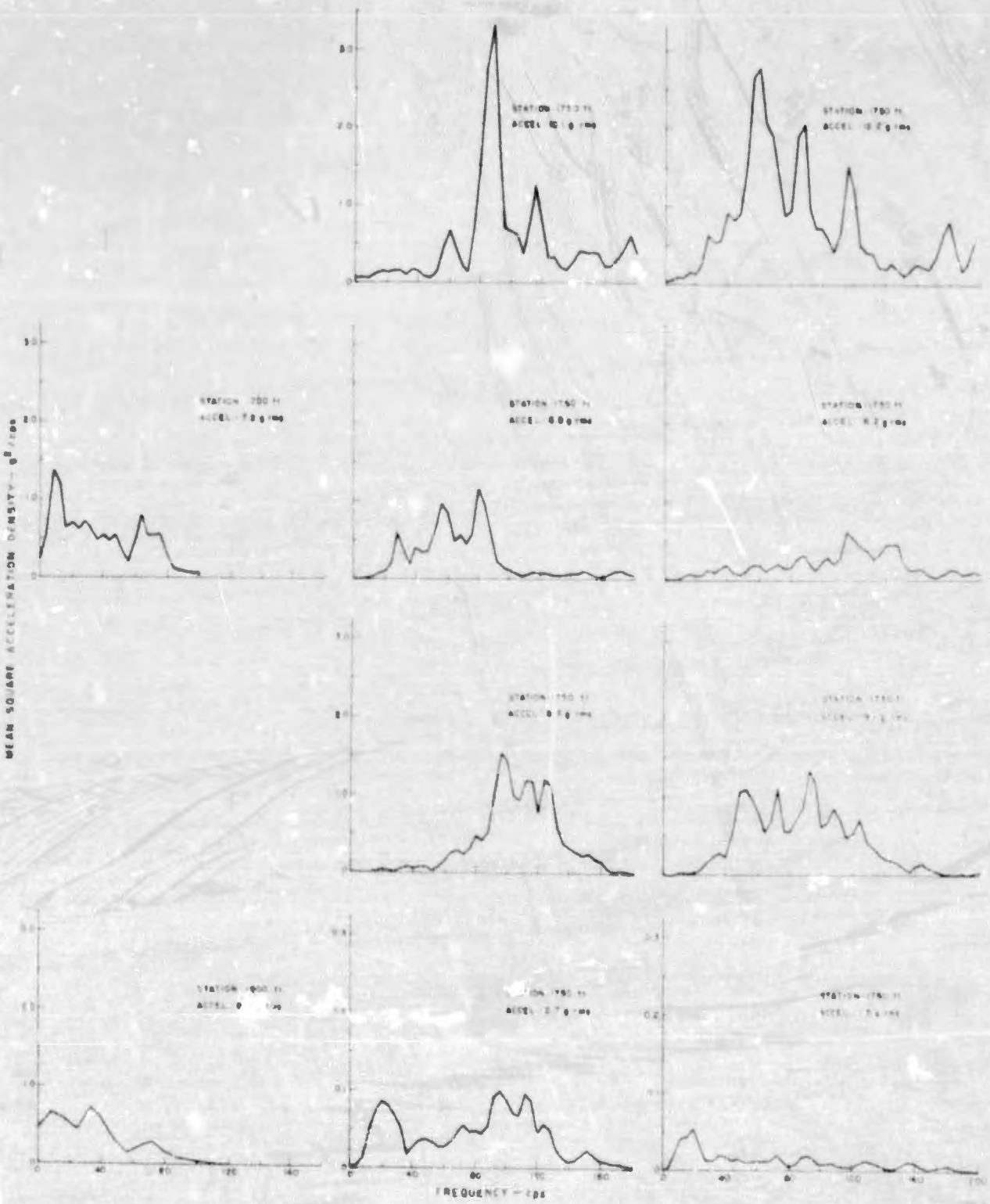

Figure 15 Spectra of Mean Square Acceleration Density for Radioplane Sled with Three Types of Slipper Mount, Vehicle Velocity Near Maximum (1265 ft/sec); Accelerometers, Vertical Direction, at Right Front Slipper (top row), Right Front Base (2nd Row), Right Rear Slipper (3rd Row), and Right Rear Base (Bottom Row). Note Different Scales.

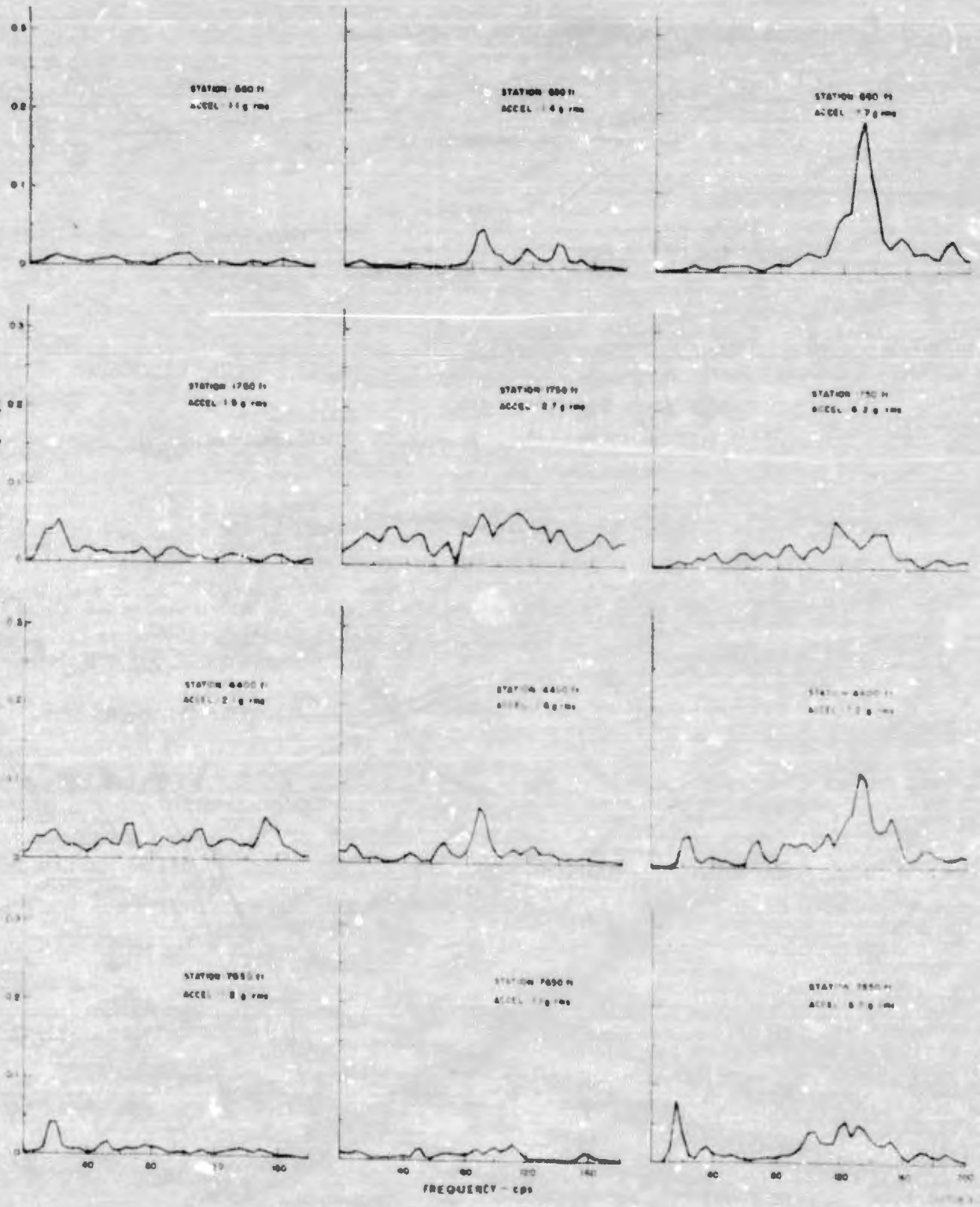

Figure 16 Spectra of Mean Square Acceleration Density at Various Track Stations for Radioplane Sled with Ski Isolators Active; Accelerometers, Vertical Direction, at Right Rear Spring Base, Center of Gravity, and Right Front Spring Base.

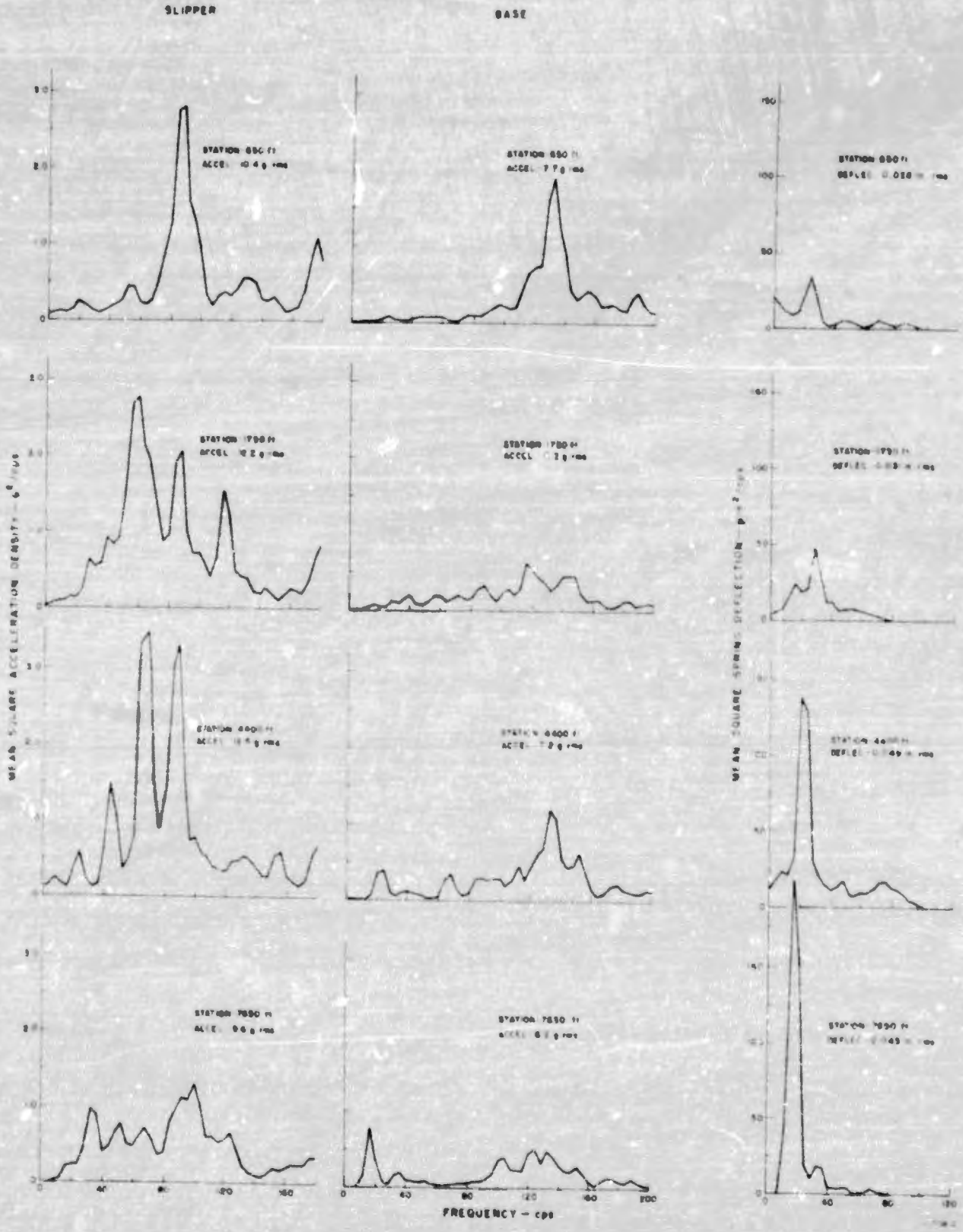

Figure 17 Spectra of Mean Square Acceleration Density and Mean Spring Deflection Density at Various Track Stations for Radioplane Sled with SRI Isolators Active; Accelerometers, Vertical Direction, at Base and Slipper Ends of Right Front Spring.

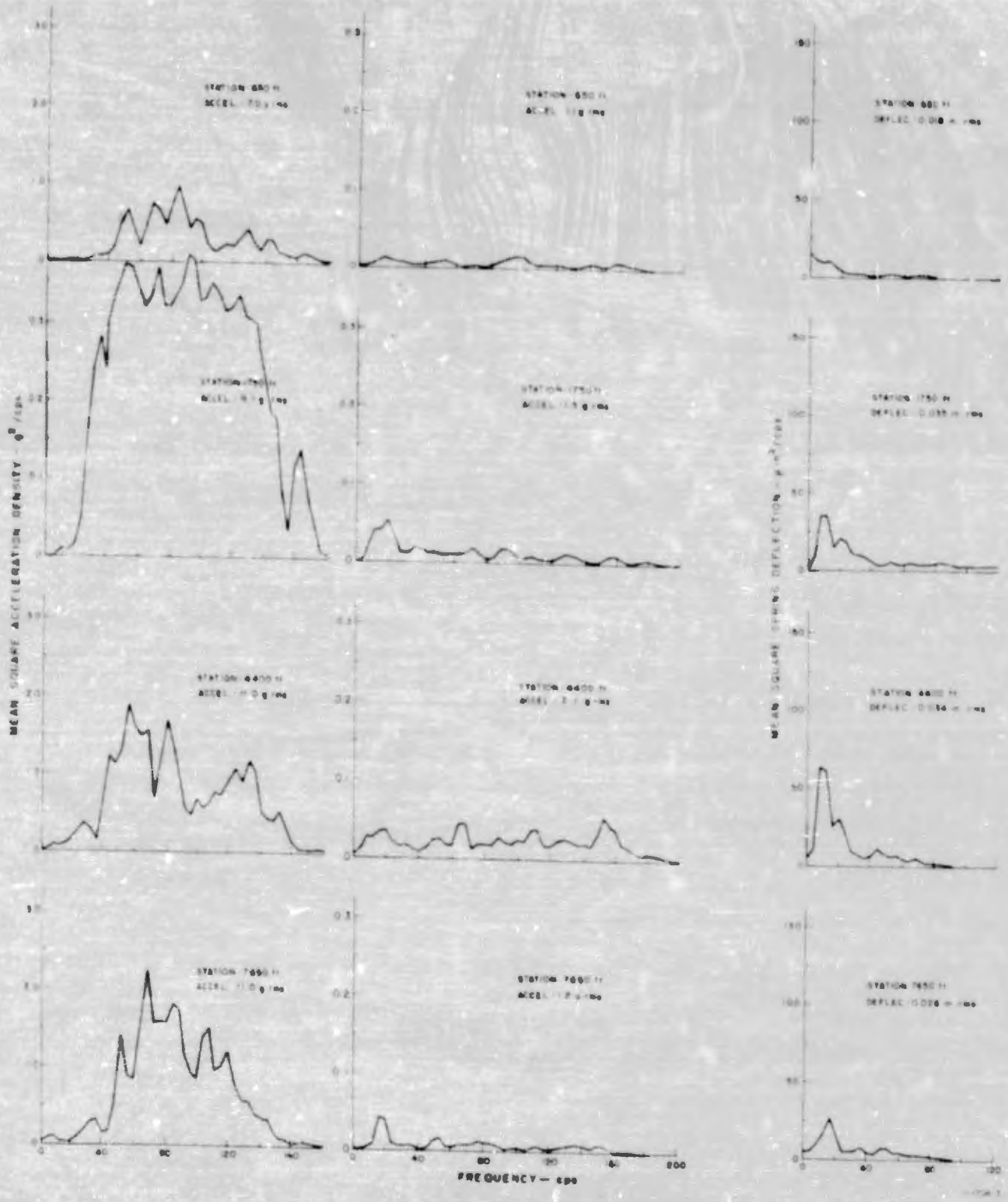

Figure 18 Spectra of Mean Square Acceleration Density and Mean Square Spring Deflection Density at Various Track Stations for Radioplane Sled with SRI Isolators Active; Accelerometers, Vertical Direction, at Base and Slipper Ends of Right Rear Spring. Note Different Scales.

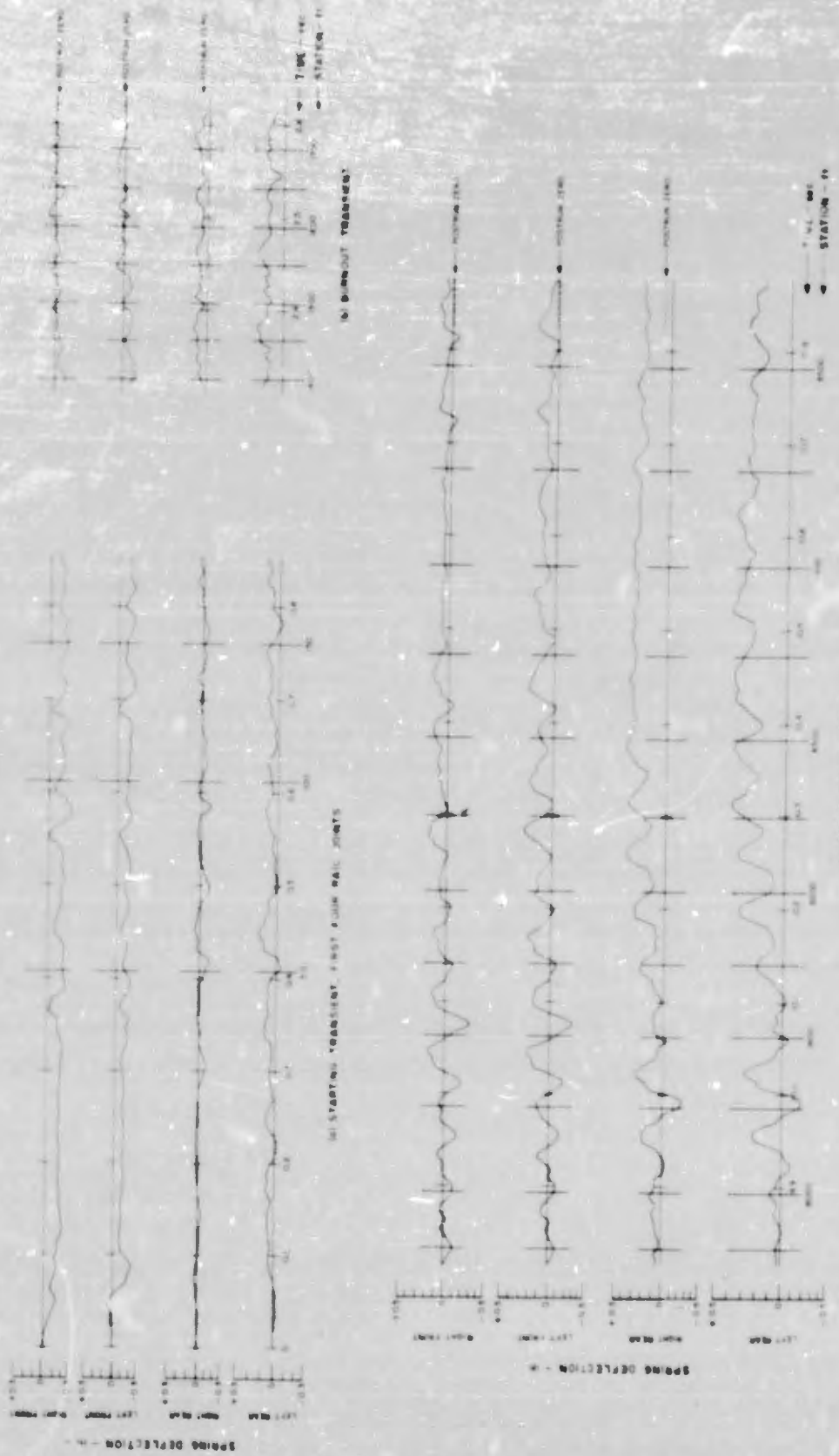

Figure 19 Spring Deflection Traces During Starting Transient, Rocket Burnout, and Water Brake Entry for Run No. 6. Baselines Represent Pre-run Zeros.

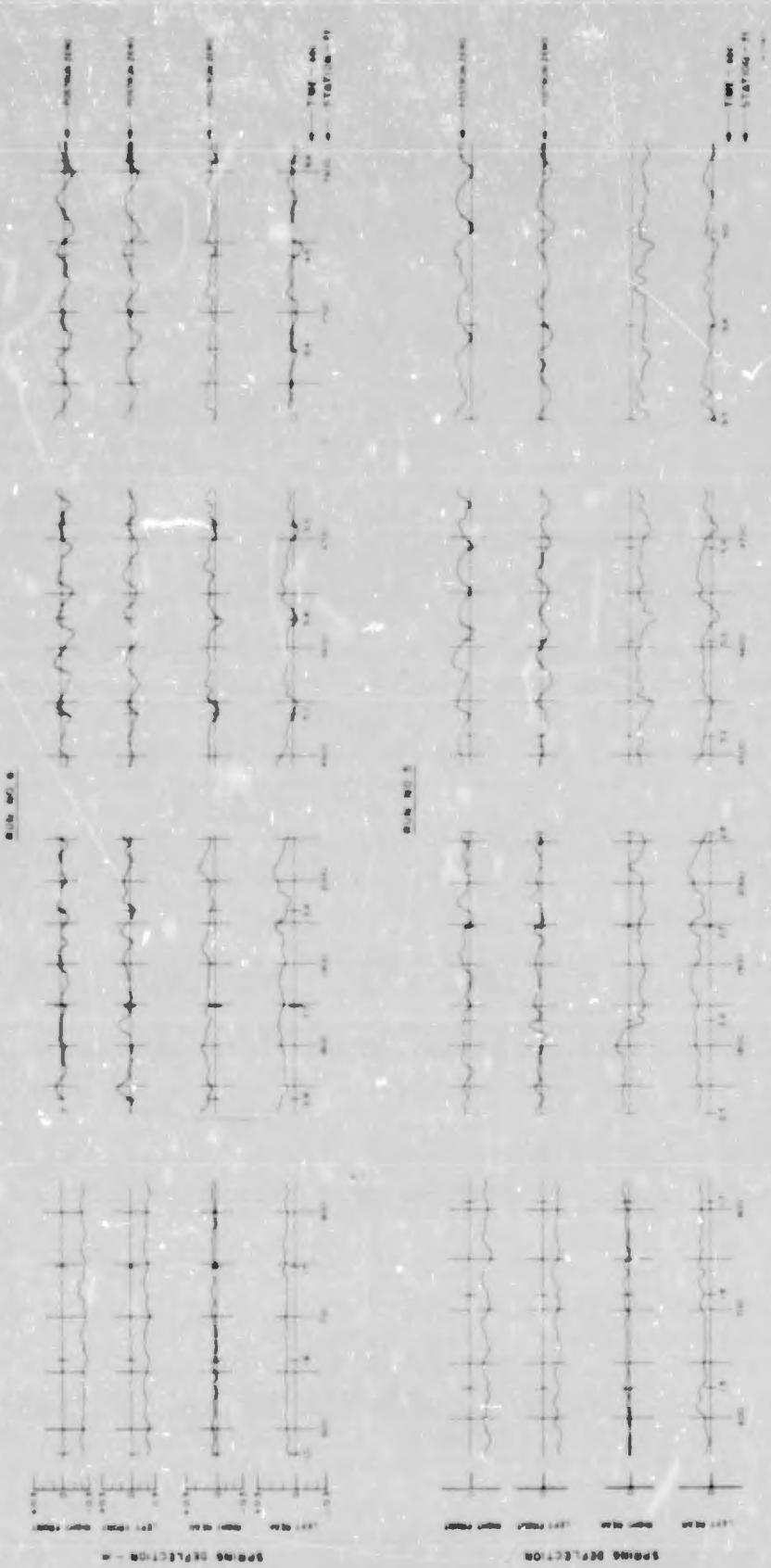

Figure 20 Spring Deflection Traces at Selected Track Stations for Run Nos. 5 and 6. Baselines represent Prerun Zeros.